The Midcontinent Rift and its mineral systems: Overview and temporal constraints of Ni-Cu-PGE mineralized intrusions

Wouter Bleeker[1*], Jennifer Smith[1], Michael Hamilton[2], Sandra Kamo[2], Dustin Liikane[2,3], Pete Hollings[4], Robert Cundari[5], Michael Easton[6], and Don Davis[2]

[1]Geological Survey of Canada, 601 Booth Street, Ottawa, Ontario K1A 0E8
[2]Jack Satterly Geochronology Laboratory, University of Toronto, 22 Russell Street, Toronto, Ontario M5S 3B1
[3]Dynamic Earth, 122 Big Nickel Road, Sudbury, Ontario 53C 5T7
[4]Department of Geology, Lakehead University, 955 Oliver Road, Thunder Bay, Ontario P7B 5E1
[5]Ontario Geological Survey, 435 James Street South, Thunder Bay, Ontario P7E 6S7
[6]Ontario Geological Survey, 933 Ramsey Lake Road, Sudbury, Ontario P3E 6B5
*Corresponding author's e-mail: wouter.bleeker@canada.ca

ABSTRACT

In an effort to better understand the spatial and temporal distributions of mineralized intrusions of the Midcontinent Rift (MCR), and what controls their style of magmatic Ni-Cu-PGE sulphide mineralization, we have compiled an overview of all known intrusions and their ages. We provide new U-Pb ages for more than ten such intrusions and/or their associated dyke systems. A number of these investigations are still in progress, and all ages should be treated as preliminary. Nevertheless, we discuss new results on the mineralized Current Lake, Sunday Lake, Tamarack, and Crystal Lake intrusions, as well as the Bovine Igneous Complex on the southern flank of the MCR. These new results, as well as improved ages for a number of the associated major dyke swarms and sill complexes (e.g. the Logan Sills), favour a relatively sharp onset of high-volume mafic-ultramafic magmatism in the MCR at ca. 1110 to 1106 Ma, although a few of the older age "outliers" remain to be tested. Mineralized intrusions are not confined to any specific magmatic pulse but are distributed through time, correlating with the major magmatic pulses at 1110–1106 Ma (e.g. Current Lake), 1104 Ma (Tamarack), of course at 1099 Ma (Duluth Complex), to as young as 1093 Ma (Crystal Lake). All these intrusions are dynamic, multi-phase, feeder-type systems. A major "post-Duluth Complex" reorganization in the magmatic plumbing system is identified starting at ca. 1097–1096 Ma, with magmatism contracting into a linear feeding zone along the northwestern shore of Lake Superior—the "north shore magmatic feeder zone" or NSMFZ—cored by the major Pigeon River dyke swarm. This feeder zone, a major magmatic fissure system, likely fed the entire lava flow field of the Portage Lake Volcanic Group, which extends to both sides of Lake Superior.

INTRODUCTION

Straddling the Canada-USA border, North America's 1.1 Ga Midcontinent Rift (MCR; Fig. 1) is one of the best preserved and most accessible Proterozoic failed intra-cratonic rift systems in the world (Wold and Hinze, 1982; Green, 1983; Van Schmus and Hinze, 1985; Hutchinson et al., 1990; Cannon, 1992; Allen et al., 1997; Miller and Nicholson, 2013; Stein et al., 2018a,b). It thus represents a pre-eminent natural laboratory for understanding the evolution of complex rift systems in cratonic settings, what generates them, what makes them fail, and the myriad of processes associated with their magmatic, sedimentary, and structural evolution, including a wide variety of mineral systems (Nicholson et al., 1992).

The MCR, with its voluminous magmatic rocks (Fig. 1, Table 1), hosts one of the largest layered intrusions in the world, the Duluth Complex (e.g. Paces and Miller, 1993), with extensive low-grade Ni-Cu-Co-PGE resources, and possibly reef-type PGE mineralization (Hauck et al., 1997; Miller, 1998; Miller et al., 2002). Some of the deposits along the western basal contact of the Duluth Complex (*see* Fig. 1) are currently in an advanced exploration and permitting stage (e.g. PolyMet, 2019) and will likely be mined in the near future. Slightly younger discrete intrusions above that contact, so-called "OUIs" (oxide-rich ultramafic intrusion; Severson et al., 2002), are rich in Fe-Ti±V oxides and are being evaluated as a Ti±V resource.

Elsewhere, both in Canada and the USA, the rift system hosts a number of smaller, localized, conduit-type mafic-ultramafic intrusions ("chonoliths") that are mineralized with higher grade Ni-Cu sulphides (e.g. Tamarack; Goldner, 2011), one of which is currently

Bleeker, W., Smith, J., Hamilton, M., Kamo, S., Liikane, D., Hollings, P., Cundari, R., Easton, M., and Davis, D., 2020. The Midcontinent Rift and its mineral systems: Overview and temporal constraints of Ni-Cu-PGE mineralized intrusions; *in* Targeted Geoscience Initiative 5: Advances in the understanding of Canadian Ni-Cu-PGE and Cr ore systems – Examples from the Midcontinent Rift, the Circum-Superior Belt, the Archean Superior Province, and Cordilleran Alaskan-type intrusions, (ed.) W. Bleeker and M.G. Houlé; Geological Survey of Canada, Open File 8722, p. 7–35. https://doi.org/10.4095/326880

being mined (Eagle; *see* Ding et al., 2010, 2012; Ripley, 2014). These intrusions remain attractive but challenging targets for mineral exploration[1]. Consequently, there is significant on-going exploration, on both sides of the Canada-US border. The large, lopolith-like, multi-phase alkaline intrusion of the Coldwell Complex, on the northeast shore of Lake Superior, has long been a target for both disseminated Cu mineralization and, more recently, for platinum group elements (PGEs; Good and Crockett, 1994; Good et al., 2015, 2017; Ames et al., 2017).

The broader rift system and its cratonic hinterland also host a wide variety of other mafic-ultramafic, alkaline, and carbonatitic intrusions (e.g. Weiblen, 1982; Sage, 1991; Wu et al., 2017), many of which have been, or are being actively explored for a range of commodities, from rare metals (Nb, e.g. the Nemegosenda intrusion) to diamonds (Kyle Lake kimberlites). The overall age range of this compositionally diverse, intracratonic magmatic activity appears to span nearly 100 Myr, from ca. 1170 Ma to ca. 1070 Ma (Davis and Sutcliffe, 1985; Davis and Paces, 1990; Heaman and Machado, 1992; Paces and Miller, 1993; Davis and Green, 1997; Heaman et al., 2004, 2007; Fairchild et al., 2017; McCormick et al., 2017; Wu et al., 2017), with the early phases of magmatic activity generally seen as precursor events to the ca. 1115–1085 Ma main magmatic phases of the rift system (*see* Miller and Nicholson, 2013, for a discussion of the evolutionary phases of the MCR).

In the final stages of its evolution, during rift inversion as a consequence of moderate regional shortening, fluid systems transported base metals, particularly Cu, but also Ag, onto the thrust-imbricated flanks of the rift, forming a variety of Cu deposits (Bornhorst and Barron, 2011), particularly in Michigan on the Keweenaw Peninsula. Elsewhere, Ag-Co-bearing mineralization and a variety of other hydrothermal veins systems (e.g. Pb-Zn-Ba veins), are spatially associated with the MCR, its intrusions, and contemporaneous faults, including, of course, the well known amethyst deposits east of Thunder Bay (e.g. Smyk and Franklin, 2007).

Finally, the MCR and its mineral systems are superimposed on the complex older setting and substrate of the rifted Superior craton margin, which was intruded by several large igneous province-scale events (e.g. the ca. 2.1 Ga Marathon magmatic event) during the Paleoproterozoic, before being overlain by variably deformed sedimentary basins hosting classic "Superior-type" banded iron formations. All these exceptional characteristics enhance the value of the MCR as an outstanding natural laboratory.

RATIONALE FOR THE PRESENT STUDY

A critical data set fundamental to any deeper understanding of this well preserved but nevertheless complex rift system, including its mineral systems, consists of precise and accurate ages of all the components that make up this rift system. Already, there is a rich literature on dating (mostly U-Pb, some Ar-Ar) of the MCR (e.g. Heaman et al., 2007 and references therein; Bleeker et al., 2018, for a recent summary). Much recent progress has focused on improving the age resolution of volcanic rocks that fill the rift, in conjunction with detailed paleomagnetic investigations, to resolve the rapidly evolving apparent polar wander path and its implications (e.g. Swanson-Hysell et al., 2014, 2019; Fairchild et al., 2017). Nevertheless, many key components of the rift system, including a wide variety of intrusions that are part of the complex plumbing system of the MCR, remain undated or have ages that require refinement, and/or have dates that are clearly puzzling outliers in the temporal framework of U-Pb ages. Some of the published U-Pb ages (e.g. Heaman et al., 2007) were obtained on limited amounts of very small baddeleyite crystals and suffer from associated complications (Pb loss and variable discordance, elevated common Pb and associated corrections, ambiguity in choice of regression line and upper intercept, subtly different systematics between baddeleyite and zircon, etc.). In some cases, there exists doubt on the exact provenance or sample location of dated samples, or whether an intrusion of interest is part of the MCR at all or possibly much older (Bleeker et al., 2018).

[1] Many of the mineralized intrusions of the MCR have sulphides with favourable Cu/Ni ratio, additional Co, and appreciable precious metal contents (PGE+Au), which adds to the overall value of their potential sulphide ores.

Figure 1 opposite page. Summary map of the Midcontinent Rift, *modified after* Miller and Nicholson (2013) and previous authors (Miller and Chandler, 1997; Weiblen, 1982, and other contributors to the volume edited by Wold and Hinze, 1982), highlighting all the rift-related intrusions. Undated or poorly dated intrusions, and (or) ages that are otherwise problematic, are shown by stars with a yellowoutline. Only a selection of ages is specifically shown on this figure (space permitting), and the reader is referred to Table 1 for additional age data and references. High-precision U-Pb ages on volcanic rocks are shown for reference (Davis and Sutcliffe, 1985; Davis and Paces, 1990; Davis and Green, 1997; Zartman et al., 1997; Schoene et al., 2006; Swanson-Hysell et al., 2014, 2019; Fairchild et al., 2017). Dyke swarms are shown using red lines and font. Newly obtained U-Pb ages as part of the present study are shown in bold red font and are summarized in Table 2. The grey band along the northwestern shore of Lake Superior is the tentative "post-Duluth Complex" 1097–1092 Ma "north shore magmatic feeder zone" (NSMFZ) discussed in this paper. Abbreviations: BIF = banded iron formation, Cgl. = Conglomerate, Fm. = Formation, Gp = group, Is. = Island, Lk. = Lake, Mt = Mount, Qte = quartzite, Twp = Township.

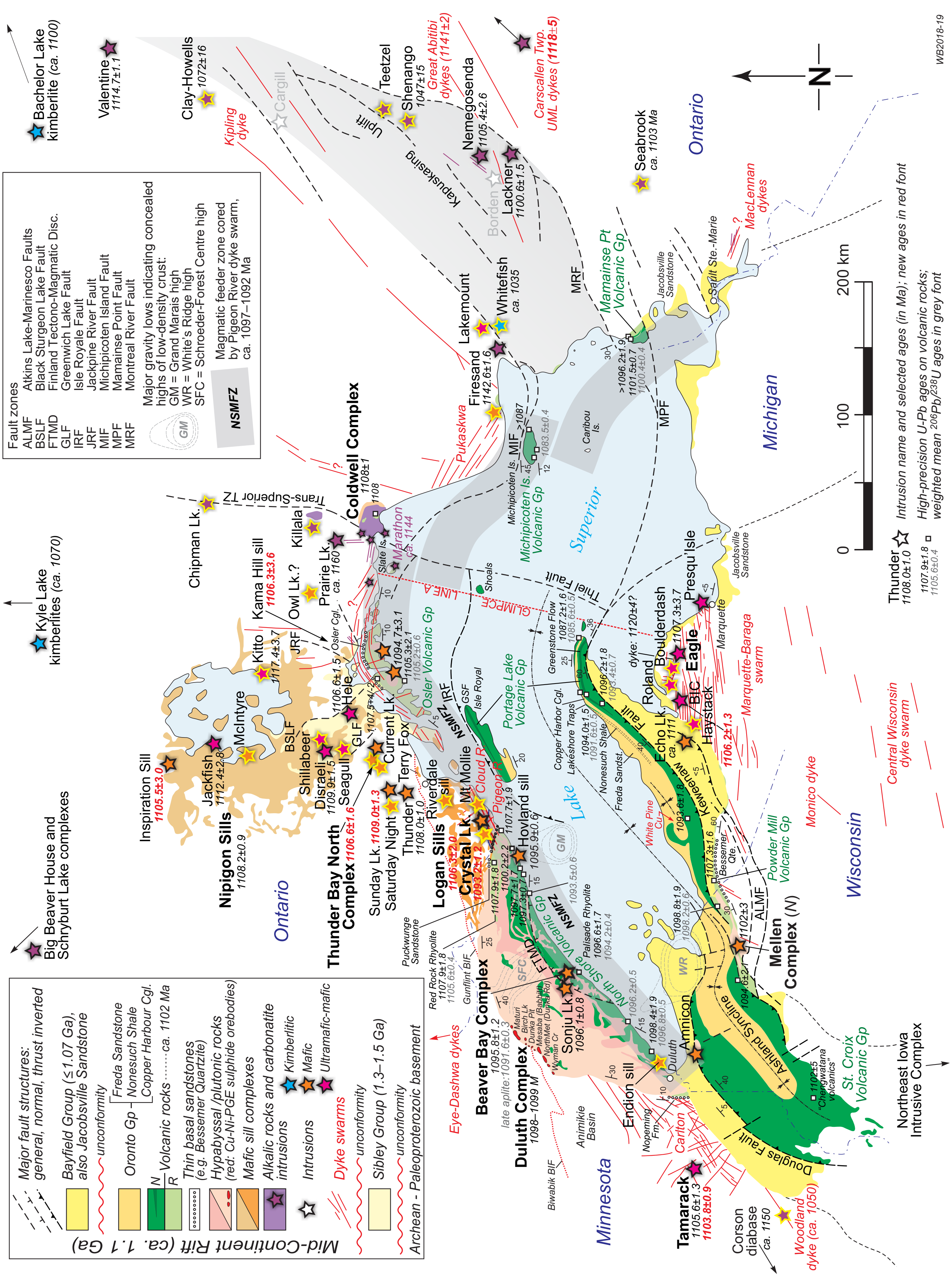
Mid-Continent Rift (ca. 1.1 Ga)
Major fault structures: general, normal, thrust inverted
Bayfield Group (≤1.07 Ga), also Jacobsville Sandstone
unconformity
Oronto Gp
Freda Sandstone
Nonesuch Shale
Copper Harbour Cgl.
N R Volcanic rocks ca. 1102 Ma
Thin basal sandstones (e.g. Bessemer Quartzite)
Hypabyssal /plutonic rocks (red: Cu-Ni-PGE sulphide orebodies)
Mafic sill complexes
Alkalic rocks and carbonatite intrusions
Intrusions
Kimberlitic
Mafic
Ultramafic-mafic
Dyke swarms
unconformity
Sibley Group (1.3–1.5 Ga)
unconformity
Archean - Paleoproterozoic basement
Fault zones
ALMF Atkins Lake-Marinesco Faults
BSLF Black Sturgeon Lake Fault
FTMD Finland Tectono-Magmatic Disc.
GLF Greenwich Lake Fault
IRF Isle Royale Fault
JRF Jackpine River Fault
MIF Michipicoten Island Fault
MPF Mamainse Point Fault
MRF Montreal River Fault
Major gravity lows indicating concealed highs of low-density crust:
GM = Grand Marais high
WR = White's Ridge high
SFC = Schroeder-Forest Centre high
NSMFZ
Magmatic feeder zone cored by Pigeon River dyke swarm, ca. 1097–1092 Ma
Thunder 1108.0±1.0 Intrusion name and selected ages (in Ma); new ages in red font
1107.9±1.8 1105.6±0.4 High-precision U-Pb ages on volcanic rocks; weighted mean ^{206}Pb/^{238}U ages in grey font
0 100 200 km
N
Lake Superior
Ontario
Michigan
Wisconsin
Minnesota
Duluth Complex 1098–1099 M
Beaver Bay Complex 1095.8±1.2
Tamarack 1105.6±1.3 1103.8±0.9
Eagle
Coldwell Complex 1108±1
Thunder Bay North Complex 1106.6±1.6
Nipigon Sills 1108.2±0.9
Logan Sills 1106.3±2.0
Crystal Lk. 1093.2±1.2
Mellen Complex (N)
Northeast Iowa Intrusive Complex
Big Beaver House and Schryburt Lake complexes
Kyle Lake kimberlites (ca. 1070)
Bachelor Lake kimberlite (ca. 1100)
Valentine 1114.7±1.1
Clay-Howells 1072±16
Kapuskasing Uplift
Nemegosenda 1105.4±2.6
Lackner 1100.6±1.5
Seabrook ca. 1103 Ma
Carscallen Twp. UML dykes (1118±5)
Great Abitibi dykes (1141±2)
MacLennan dykes
Marquette-Baraga swarm
Central Wisconsin dyke swarm
Monico dyke
Eye-Dashwa dykes
Woodland dyke (ca. 1050)
Mamainse Pt Volcanic Gp
Michipicoten Is. Volcanic Gp
Osler Volcanic Gp
Portage Lake Volcanic Gp
Powder Mill Volcanic Gp
North Shore Volcanic Gp
St. Croix Volcanic Gp
Ashland Syncline
Douglas Fault
Keweenaw Fault
Thiel Fault
Trans-Superior TZ
GLIMPCE LINE A
Sault Ste.-Marie
Duluth
Marquette
WB2018-19

Table 1. Listing of Midcontinent Rift-related intrusions, updated from Bleeker et al. (2018).

#	Intrusive Unit	Age (Ma)	Type of Age	Key References	Main Rock Types	Comments and Questions
	MCR-related dyke swarms:					
1	Great Abitibi dykes	1141±2	U-Pb, bd, wm7/6 age	Krogh et al., 1987	Olivine diabase, gabbro, monzodiorite	Giant swarm, only one dyke dated
	Ultramfic lamprophyres:					
2	Ultramafic "Marathon dykes" (e.g., McKellar Harbour dyke)	ca. 1144 1145+15/-10	K-Ar U-Pb, prv	Platt and Mitchell., 1979, 1982; Platt et al., 1983; Queen et al., 1996	Ultramafic lamprophyre	Kimzeyite garnet in some dykes Age uncertainty allows link to Prairie Lake Complex
3	Lamprophyre dykes, Kapuskasing Uplift	ca. 1144	Ar-Ar	Queen et al., 1996	Ultramafic lamprophyre	Also age overlap with Abitibi dykes
4	Lamprophyre dykes, Carscallen Twp.	ca. 1118	Ar-Ar	This study	Ultramafic lamprophyre	Ultramafic lamprophyre intersected in core, west of Timmins
5	Woodland dyke, Minnesota (~060°)	ca. 1050	Ar-Ar	This study; T. Boerboom, pers. comm., 2016	Lamprophyre	Large, ~8 m wide lamprophyre dyke, reversely magnetized
	Various mafic dyke sets:					
6	ESE-trending diabase and lamprophyre dykes east of Sault Ste. Marie	undated		This study	Thin (ultramafic) lamprophyre dykes cut by slightly younger diabase dykes	Fresh lamprophyre and lamprophyre-diabase association is typical for MCR
7	ENE-trending dykes north of Wawa	undated		This study	Diabase	Trend ~070°, ~4–5 m wide, exposed along Hwy 17
8	NNE-trending dykes east of Coldwell	undated		OGS 1991a, Map 2543	Diabase	Distinct from Marathon dykes?
9	NNW-trending dykes west of Coldwell	undated		OGS 1991a, Map 2543; this study	Diabase	Observed in road outcrops; reversely magnetized
10	Pukaskwa dykes (~315°)	undated		OGS 1991a, Map 2543; Weiblen, 1982; Green et al., 1987	Diabase	Could be confused with parallel Matachewan dykes
11	NW- to N-trending dykes, Nipigon area	undated		OGS 1991b, Map 2542; Osmani, 1991; this study	Diabase	Some have been shown to be Marathon swarm dykes
12	E- to NE-trending diabase and lamprophyre east of Nipigon	undated		This study	Thin (ultramafic) lamprophyre dykes cut by slightly younger diabase dykes	Fresh lamprophyre and lamprophyre-diabase association is typical for MCR
13	E-trending diabase dykes cutting Osler Group flows	undated, 1096?		Giguerre, 1975; this study	Diabase dykes 3–30 m in width	Dykes cut and chilled against Osler Group basalt flows, and dip steeply north; tilted with flows; probably equivalents of Pigeon River dyke, and feeders to Portage Lake Group
14	Thin WNW-trending dykes north of Atikokan, cutting Eye-Dashwa pluton	1143±27	K-A	Osmani, 1991; Stone et al., 1992	Thin diabase dyke, trend ~290°	
	NW-trending dykes:					
15	Cloud River dykes (~330°), near Crooks	1109.2±4.2 1109.2±2.9	U-Pb, bd, wm6/8 age, n=2 U-Pb, bd, n=3	Hollings et al., 2010; Cundari, 2012 This study	Diabase Diabase, sparsely plagioclase megacrystic in centre	 ~80 m NW-trending (~318°) Cloud River dyke cut by ENE-trending Pigeon River dykes
16	NW-trending dyke at Mt. Josephine	1099.0±1.2	U-Pb, zr and bd, wm7/6 age, n=5	This study	Diabase	~100–150 m wide dyke, vertical, trend 330°
	Pigeon River swarm and parallel dykes:					
17	Pigeon River dyke (~070°), Crooks Twp. "Rita Bolduc dyke"	1141±20 1096.9±1.9	U-Pb, zr and bd, disc.	Heaman et al., 2007 This study	Diabase, gabbro	Higly discordant data, age interpretation likely too old
18	Arrow River dyke (~080°), Devon Twp.	1078±3 1096±12	U-Pb, bd, reverse disc., n=1	Heaman et al., 2007 This study	Diabase	Arrow River, Devon Township
19	Mount Mollie dyke (080-090°)	1109.3±6.3 1096.3±1.4	U-Pb, bd, wm7/6 age, n=2 U-Pb, zr and bd, u. intercept, n=6	Smyk and Hollings, 2009; Hollings et al., 2010 This study	Diabase, gabbro to leucogabbro, granophyre	Uncertainty on sample location; age in conflict with feeder to Crystal Lake Intrusion Mount Mollie dyke probably a member of the Pigeon River swarm
	Other dyke swarms:					
20	Carlton dykes (~030°, multiple trends)	undated		Weiblen, 1982; Green et al., 1987; Miller and Nicholson, 2013	Diabase	Multiple trends, i.e. likely more than one swarm
21	Marquette-Baraga dykes (080°)	ca. 1120±4	U-Pb bd, n=3, disc., u. intercept	Weiblen, 1982; Green et al., 1987; Miller and Nicholson, 2013; *see* Dunlop, 2013, for baddeleyite date	Diabase	Multiple trends, i.e. likely more than one swarm
22	NE-trending dykes south of MCR e.g., Monico dyke	undated		K. Schultz, pers. comm., 2019		Several NE-trending dyke below the ridge of the Bessemer Quartzite, also the Monico dyke farther south
23	Central Wisconsin dyke swarm	undated		Osmani, 1991		
24	NE-trending dykes, northeast Iowa	undated		Drenth et al., 2015		Associated with Northeast Iowa Intrusive Complex; some appear reversely magnetized
	Various sills and sill complexes:					
	"Nipigon Sills", Nipigon area:					
25	Nipigon Sills	1109+4/-2 1108.2±0.9	U-Pb, zr (and bd), n=4 U-Pb, zr, u. intercept, recalculated	Davis and Sutcliffe, 1985; *see also* Krogh et al., 1987 *see* Davisand Green, 1997	Diabase, pegmatitic gabbro, granophyre	These were referred to as "Logan Sills" by Davis and Sutcliffe, 1985
26	Havoc Lake diabase (HAV02-02)	1110.1±2.5	U-Pb, bd, wm7/6, n=4	Heaman et al., 2007	Diabase	
27	Muskrat Lake diabase (ML01-01)	1112.7±2.4	U-Pb, bd, wm7/6, n=2	Heaman et al., 2007	Diabase	
28	Grand Bay diabase (GB01-01)	1114.4±8.3	U-Pb, bd, disc., scattered data	Heaman et al., 2007	Diabase	
29	North Bay diabase (LN08)	1110.1±2.1	U-Pb, bd, wm7/6, n=2	Heaman et al., 2007	Diabase	
30	Gull River troctolite (GR01-01)	1111±15	U-Pb, bd, wm7/6, n=2	Heaman et al., 2007	Troctolite	
31	South Bay diabase (LN139)	1106.8±1.9	U-Pb, zr, reversly disc., wm7/6, n=2	Heaman et al., 2007	Diabase	
32	Kama Hill, upper sill (KH10)	1008±29	U-Pb, zr, highly disc., n=2	Heaman et al., 2007	Diabase	Upper intercept through highly disc. zircon data
33	Inspiration (04RME-3210)	1159±33 1105.5±3.0	U-Pb, bd, disc., n=2, u. intercept U-Pb, bd, wm7/6, n=3	Heaman et al., 2007 This study	Diabase, gabbro	Upper intercept from 2 disc. baddeleyite fractions, likely too old Redated, see new age in line with other Logan and Nipigon sills
34	McIntyre	1100.8±4.4	U-Pb, bd, wm7/6 age, n=1	Heaman et al., 2007	Diabase	More likely to be ca. 1110 Ma based on wm6/8 age
	"Logan Sills", Thunder Bay area:					
35	Logan Sills	1114.7±1.1 1106.3±2.0	U-Pb, bd, 3.5-4.1% disc, wm7/6 U-Pb, zr and bd, u. intercept, n=5	Heaman et al., 2007 This study	Diabase	Clustered discordant data, age interpretation likely too old
36	Terry Fox sill	undated			Diabase, plagioclase phyric near roof contact	Interesting upper porphyry, with abundant xenoliths, melted roof rocks?
37	Riverdale	undated		Hollings et al., 2010; P. Hollings, pers. comm., 2017	Diabase, compositionally distinct	

Table 1 continued.

#	Intrusive Unit	Age (Ma)	Type of Age	Key References	Main Rock Types	Comments and Questions
	Intrusions in Minnesota, likely related to Logan Sills:					
38	Nathan's Layered Series	1106.9±0.6	U-Pb, zr, wm7/6, n=5	Weiblen et al., 1972; Paces and Miller, 1993	Olivine gabbro	Reversely magnetized, age suggest link with Logan Sills
39	Swamper Lake monzogabbro	1107.0±1.1	U-Pb, zr, wm7/6, n=3	Davis and Green, 1997	Monzogabbro	Reversely magnetized, age suggest link with Logan Sills
40	Cucumber Lake granophyre	1106.8±2.8	U-Pb, zr, u. intercept	Vervoort and Wirth, 2004; Vervoort et al., 2007	Granophyre	Reversely magnetized
41	Misquah Hills granophyre	1106.0±4.8	U-Pb, zr, u. intercept	Vervoort and Wirth, 2004; Vervoort et al., 2007	Granophyre	
42	Whitefish Lake granophyre	1109.4±5.1	U-Pb, zr, u. intercept	Vervoort and Wirth, 2004; Vervoort et al., 2007	Granophyre	
43	Mount Weber granophyre	1106.2±3.6	U-Pb, zr, u. intercept	Vervoort and Wirth, 2004; Vervoort et al., 2007	Granophyre	
44	Greenwood Lake granophyre	1106±3	U-Pb, zr, u. intercept	Vervoort and Wirth, 2004	Granophyre	
	Ultramafic intrusions:					
45	Kitto	1117.5±3.7	U-Pb, bd, wm7/6, n=2	Sutcliffe, 1986; Hart et al., 2002; Heaman et al., 2007; Larmaan, 2007	Peridotite, olivine websterite, and pyroxenite	Interstitial sulphides along basal contact and in websterite
46	Kitto diabase	1110.8±4.3	U-Pb, bd, disc., u. intercept	Heaman et al., 2007	Diabase thought to intrude Kitto ultramafic body	
47	Seagull	1112.8±1.4	U-Pb, bd, complex results	Heggie, 2005; Hart and Macdonald, 2007; Heaman et al., 2007	Dunite, peridotite to gabbro	Disseminated sulphides along basal contact, and reef-type PGE horizons
48	Jackfish	1112.4±2.8	U-Pb, bd, wm6/8 age, n=2	Heaman et al., 2007; Hollings et al., 2007	Melagabbro to peridotite core surrounded by olivine gabbro	
49	Disraeli	1109.9±1.4	U-Pb, bd, wm7/6, n=2	Hart and Magyarosi, 2004; Hart and Macdonald, 2007; Heaman et al., 2007	Peridotite to wehrlite core, with olivine gabbro marginal zone	Good baddeleyite age
50	Hele	1106.6±1.5	U-Pb, bd, wm7/6, n=2	Heaman et al., 2007; Hollings et al., 2007	Peridotite and wehrlite, interlayered with olivine gabbro	Minor sulphides in peridotite
51	Shillabeer	undated		Hollings et al., 2007	Ultramafic rocks	
	Thunder Bay North Complex:					
52	Current Lake	1120±23	U-Pb (unpubl.), no details	Smyk and Hollings, 2009; Chaffee, 2015	Feldspathic dunite to olivine melagabbro	Disseminated sulphides in peridotite, net-textured to massive sulphide in conduit
		1106.6±1.6	U-Pb, zr and bd, u. intercept, n=4	This study		
53	Steepledge Lake	undated		Thomas et al., 2011; D'Angelo, 2013	Peridotite to olivine gabbro	Basal peridotite hosts disseminated sulphides
54	Lone Island Lake	undated				
	Other intrusions:					
55	Thunder	1108.0±1.0	U-Pb, zr (bd), CA-ID-TIMS, conc.	Trevisan, 2014; Trevisan et al., 2015	Feldspathic peridotite, melagabbro, and upper massive gabbro	Disseminated sulphides in basal ultramafic rocks
56	Sunday Lake	1109.0±1.3		Flank, 2017; this study	Peridotite to monzogabbro (diorite)	Disseminated sulphides in basal ultramafic rocks
57	Tamarack Intrusive Complex	1105.6±1.3	U-Pb, bd, slightly disc.	Goldner, 2011; Taranovic et al., 2015, 2016	Peridotite to gabbro	Net-textured to massive sulphide; disseminated sulphides thoughout
		1103.8±0.9	U-Pb, zr, concordia age	This study, new age on pegmatitic gabbro of "southern bowl"		
58	Saturday Night	*in progress*		This study	Peridotite to monzogabbro (diorite)	Disseminated sulphides in basal ultramafic rocks
59	Crystal Lake Intrusion	1099.6±1.2	U-Pb, bd, wm7/6, n=2	Cogulu, 1993a,b; Heaman et al., 2007;	Vari-textured gabbro, troctolite, chromite layers	Some controversy on what part of the complex was dated
		1093.1±1.2	U-Pb, zr and bd, wm7/6, n=4	Smith et al., 2020; this study		
60	Blake Township Gabbro	1091.0±4.5	U-Pb, bd, wm6/8, 7/5 ages, n=2	Heaman et al., 2007	Gabbro	Blake Township
61	"Rainy River intrusion"	undated		W. Bleeker, unpublished observations on core	Peridotite-gabbro, metamorphosed, mineralized	Metamorphosed, cut by Fort Frances dyke, Archean; not MCR-related
	Younger gabbro intrusions in Osler Group:					
62	Moss Lake Gabbro	1094.7±3.1	U-Pb, bd, wm6/8, 7/5 ages, n=2	Heaman et al., 2007	Gabbro	Black Bay Peninsula, intrusive units emplaced in Osler Group
63	St. Ignace Island Complex Gabbro	1089.2±3.2	U-Pb, zr, unpubl.	Smyk et al., 2006	Gabbro	St. Ignace Island, intrusive units emplaced in Osler Group
	Duluth Complex and related intrusions, Minnesota:					
64	Duluth Complex	1099.0±0.6	U-Pb, zr, wm7/6, n=5	Paces and Miller, 1993; *see also* Hoaglund et al., 2010	Gabbroic anorthosite	
65	Duluth Complex	1099.1±0.5	U-Pb, zr, wm7/6, n=6	Paces and Miller, 1993	Gabbroic anorthosite	
66	Duluth Complex	1098.6±0.5	U-Pb, zr, wm7/6, n=8	Paces and Miller, 1993	Olivine gabbro	
67	Duluth Complex	1099.3±0.3	U-Pb, zr, wm7/6, n=6	Paces and Miller, 1993	Olivine ferrogabbro	
68	Kenwood Avenue granite	1098.2±1.4	U-Pb, zr, wm7/6, n=4	Davis and Green, 1997	Granite	One of the youngest phases clearly associated with the Duluth Complex
69	Pine Mountain granophyre	1095.3±3.8	U-Pb, zr, u. intercept	Vervoort and Wirth, 2004; Vervoort et al., 2007	Granophyre	
70	Eagle Mountain	1098.6±3.8	U-Pb, zr, u. intercept	Vervoort and Wirth, 2004; Vervoort et al., 2007	Granophyre	
71	Finland granophyre	1098.2±5.5	U-Pb, zr, u. intercept	Vervoort and Wirth, 2004; Vervoort et al., 2007	Granophyre	
72	Sonju Lake Intrusion (part of BBC)	1096.1±0.8	U-Pb, bd, wm7/6	Paces and Miller, 1993	Ferrodiorite	
73	Beaver Bay Complex (BBC), Silver Bay Intr.	1095.8±1.2	U-Pb, zr and bd, wm7/6, n=6	Paces and Miller, 1993	Granophyric ferrogabbro	
74	Intrusive aplites in Silver Bay Intr.	1091.6±0.3	U-Pb, zr, CA-TIMS, wm6/8 age	Fairchild et al., 2017	Aplite within granophyre	$^{206}Pb/^{238}U$ ages on multiple chemically abraded zircons
75	Wilson Lake ferrogabbro	1095.8±0.9	U-Pb, zr and bd, wm7/6, n=6	Hoaglund et al., 2010	Ferrogabbro	
76	Hovland Sill	1095.9±0.6	U-Pb, bd, wm7/6, n=6	Boerboom et al., 2014	Gabbro to granophyre	UTM: 722714E, 5301024N
77	Endion Sill	undated		Miller, 2016	Gabbro to granophyre	Exposed along the shore in Duluth
	Mafic-ultramafic intrusions south of Lake Superior:					
78	Amnicon gabbro intrusion	undated		Grout, 1918; J. Miller, pers. comm., 2019	Gabbro	
	Mellen Intrusive Complex:					
79	Mineral Lake Intrusion	1102.8±2.8	U-Pb, zr, wm7/6 age, n=2	Zartman et al., 1997	Olivine gabbro, ferrogabbro, granophyre, and late granite	Basal mineralization confined to Mineral Lake Intrusion

Table 1 continued.

#	Intrusive Unit	Age (Ma)	Type of Age	Key References	Main Rock Types	Comments and Questions
	Mellen Intrusive Complex continued:					
80	Mineral Lake Intrusion	1102.1±3.5	U-Pb, zr, u. intercept	Zartman et al., 1997	Granophyre	Wisconsin
81	Mellen Complex	1101.5±2.9	U-Pb, zr, u. intercept	Zartman et al., 1997	Granite	Wisconsin
82	Echo Lake	1110.8±1.5	U-Pb, unpubl.	Cannon and Nicholson, 2001; Koerber and Thakurta, 2017; S. Nicholson, pers. comm., 2018	Peridotite, troctolite, gabbro	Localized PGE horizons associated with disseminated sulphides
83	Bovine Igneous Complex (BIC)	1106.2±1.3	U-Pb, bd, u. intercept, n=3	Foley, 2011; Donoghue et al., 2014; this study	Feldspathic wehrlite overlain by melatroctolite and olivine gabbro	Basal, disseminated to locally massive sulphides, also reef-style PGE horizons
84	Roland Lake	undated		Dunlop, 2013	Feldspathic peridotite to pyroxenite	Minor sulphide mineralization, extent yet to be determined
85	Boulderdash	undated		Dunlop, 2013	Troctolite, melatroctolite	Minor sulphide mineralization, extent yet to be determined
86	Eagle	1107.3±3.7	U-Pb, bd, wm7/6 age	Ding et al., 2010, 2012; *see also* Ripley, 2014; Clow et al., 2017	Feldspathic peridotite sheet, underlain by melatroctolite and olivine gabbro	Relationship to Eagle East?
87	Eagle East	undated		As for Eagle, *see above*	Melatroctolite	High-grade massive to semi-massive sulphides concentrated above keel
	Coldwell Complex and nearby intrusions:					
88	Coldwell Complex	1108±1	U-Pb, zr, u. intercept	Mitchell et al., 1983, 1993; Heaman and Machado, 1992; Good et al., 2015, 2017	Gabbro, ferroaugite syenite, nepheline syenite, quartz syenite	Disseminated Cu and PGE mineralization in vari-textured Two Duck Lake gabbro; remnants of pre-intrusive basalts, preserved as hornfelsed roof pendants (xenoliths)
	Eastern marginal gabbro, Centre 1 (CL7)	1107+2/-1	U-Pb, bd and zr, u. intercept	Heaman and Machado, 1992	Gabbro	
	Two Duck Lake gabbro, Centre 1 (86CL1)	1108±1	U-Pb, bd and zr, u. intercept	Heaman and Machado, 1992	Coarse vari-textured gabbro	
	Syenite, Centre 1	ca. 1108	U-Pb, zr, some scatter	Heaman and Machado, 1992	Syenite	
	Nepheline syenite, Centre 2 (CL22)	1109+8/-4	U-Pb, zr and ti, disc.	Heaman and Machado, 1992	Nepheline syenite	
	Granite, Centre 3	≥1102	U-Pb, zr, disc.	Heaman and Machado, 1992	Granite	Centre 3 could be as young as 1102–1103 Ma
89	Prairie Lake	ca. 1163	U-Pb, bd and zr	Rukhlov and Bell, 2010; Wu et al., 2017	Pyroxenite, ijolite, carbonatite, syenite	Early precursor alkaline magmatism; plume incubation?
90	Killala	1050±35 1185	Rb-Sr K-Ar	Bell and Blenkinsop, 1980; Sage, 1988d Currie, 1976	Syenite, nepheline syenite, olivine gabbro, larvikite	Minor Nb and Ni-Cu sulphide mineralization
91	Owl Lake	undated				
92	Chipman Lake	1022±31	K-Ar	Sage, 1985	Carbonatite and lamprophyre dykes	Emplaced along the Trans-Superior Tectonic Zone
93	"Marathon dykes" (see under dykes)	ca. 1144				
	Ultramafic intrusions near Wawa:					
94	Firesand	1142.6±1.6 1019–1098	U-Pb, kmz K-Ar	Sage, 1988e, 1991; Rukhlov and Bell, 2010 Gittins et al., 1967	Carbonatite and related alkalic rocks	
95	Lakemount (a.k.a. Sunrise)	undated			Peridotite; basal Ni-Cu mineralization	Relation to MCR uncertain
	Alkaline and carbonatite intrusion east of Lake Superior:					
96	Seabrook Lake	1113±36	K-Ar	Gittins et al., 1967; Sage, 1988a	Carbonatite, mafic breccias, ijolite, syenite	Minor Nb mineralizaton
97	Lackner Lake	1100.6±1.5	U-Pb, bd, disc., n=3, intercept	Heaman et al., 2007	Carbonatite, ijolite and associated magnetite-apatite bodies, nepheline syenite	Minor Nb mineralizaton
98	Nemegosenda	1105.4±2.6	U-Pb, zr, u. intercept, n=3	Sage, 1987a; Heaman et al., 2007	Carbonatite, ijolite, nepheline syenite, syenite, gabbro	Nb mineralization
99	Shenango	1047±15	Rb-Sr	Bell and Blenkinsop, 1980; Sage, 1987b	Diorite, syenodiorite, monzonite and quartz monzonite	
100	Teetzel	1155±45	K-Ar	Currie, 1976; Weiblen, 1982		
101	Clay-Howells	1075±15	Rb-Sr	Bell et al., 1982; Sage, 1988b	Pyroxene syenite, intruded by magnetite-rich carbonatite dykes	REE, Nb and Fe (magnetite) mineralization
102	Valentine	1114.7±1.1	U-Pb, bd, u. intercept	Sage, 1988c; Rukhlov and Bell, 2010	Carbonatite	Widespread but sub-economic Nb and P mineralization
	Alkaline and carbonatite intrusion in NW Ontario:					
103	Big Beaver House	1093±2 1109±61	U-Pb, bd, disc., n=1 K-Ar, bi	Sage, 1991; Rukhlov and Bell, 2010 Sage, 1987c	Alkaline ultramafic rocks, carbonatite	Single 1.4% discordant bd fraction
104	Schryburt Lake	1084±3	U-Pb, bd, disc., n=2, intercept	Sage, 1988f, 1991; Rukhlov and Bell, 2010	Ultramafic lamprophyre, carbonatite	Weighted mean of the 2 bd analyses is 1083.0±1.2 Ma
	Kimberlites:					
105	Kyle Lake kimberlites	ca. 1070	U-Pb, prv, single analysis	Heaman et al., 2004	Kimberlite, diamondiferous	Northern Ontario, underneath Paleozoic cover
106	Whitefish Lake	1035±13 (1097±7)	Rb-Sr, phl	Kaminsky et al., 2000	Kimberlite, micaceous, diamondiferous	North east of Wawa, four kimberlite pipes
107	Bachelor Lake	1104±17	Rb-Sr, phl	Alibert and Albarede, 1988	Kimberlite	Western Quebec, underneath glacial till
	Distal events:					
108	Northeast Iowa Intrusive Complex	undated		Drenth et al., 2015	Various intrusion, both mafic and felsic	
109	Corson diabase	ca. 1150	U-Pb, bd	McCormick et al., 2017	Olivine diabase	Near border of South Dakota and Minnesota
110	Texaco-Poersch core, Kansas	1097.5±3.0	U-Pb, zr	Van Schmus, 1992	Gabbro	Kansas
111	Moore Lake gabbro	1109±2	U-Pb, bd and zr	French et al., 2002	Gabbro, diabase	Gabbro sills intruding the Athabasca Basin, Saskatchewan
112	Douglas River diabase dyke	1165±17	U-Pb, bd, in situ SIMS dating	Bleeker and Chamberlain, 2015	Diabase	Diabase dykes intruding the Athabasca Basin, Saskatchewan
113	SW USA Diabase Province	1115–1080	U-Pb, bd, various methods	Bright et al., 2014, and references therein	Diabase and gabbro sills, layered intrusion	Possibly a distal expression of the same MCR mantle upwelling?
114	Pahrump sills	1087±3	U-Pb, bd	Heaman and Grotzinger, 1992	Diabase, gabbro	Diabase sills in Parump Group, southern California
115	Salla dyke	1122±7	U-Pb, zr	Lauerma, 1995; Salminen et al., 2009	Medium- to coarse-grained diabase	A single large (distal), NE-trending diabase dyke, cutting across northern Karelia
116	Umkondo LIP, Kalahari craton	1112–1106	U-Pb, bd and zr	Hanson et al., 2004	Diabase, gabbro	Numerous diabase dykes and sills across Southern Africa

Notes: This is a compilation in progress; some unpublished information is currently included. In red, intrusions worked on during this study.
Abbreviations: bd = baddeleyite, bi = biotite, conc. = concordant, disc. = discodant, kmz = kimzeyite, n = number of analyses included, PGE = platinum group elements, phl = phlogopite, prv = perovskite, REE = rare earth elements, ti = titanite, u. intercept = upper intercept, wm6/8 = weighted mean $^{206}Pb/^{238}U$ date, wm7/6 = weighted mean $^{207}Pb/^{206}Pb$ date, zr = zircon.

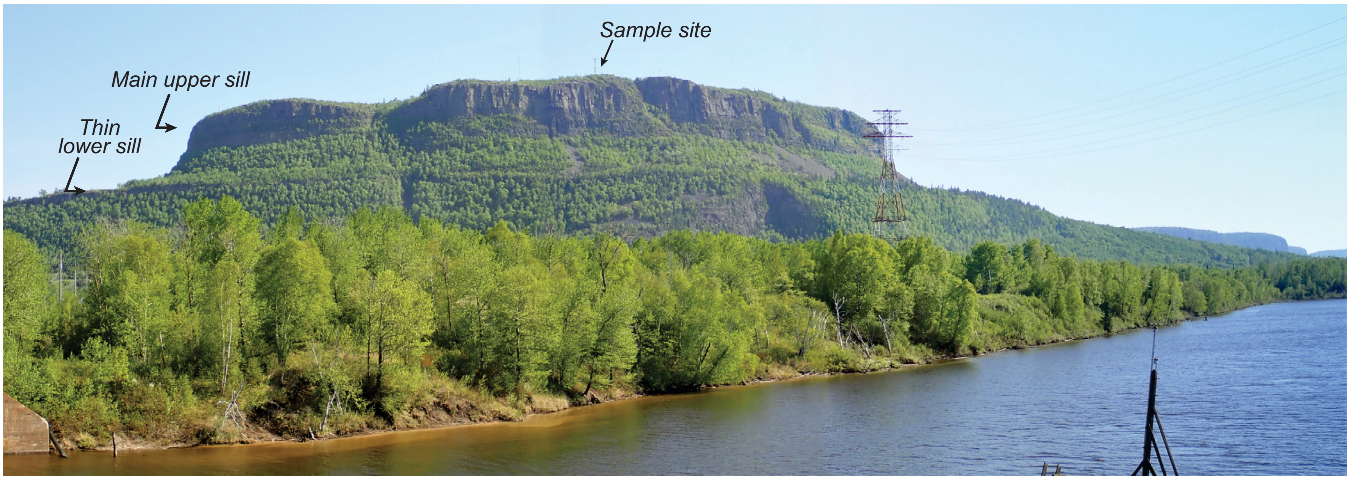

Figure 2. View of the iconic Logan Sills (s.s.) overlooking the Kaministiquia River and the city of Thunder Bay. Two sills are visible, having intruded mudstones and thinly bedded turbiditic wackes of the ca. 1.85 Ga Rove Formation, Animikie Basin: an upper main sill capping the mesas, and a thin lower sill forming a minor ledge in the trees. William Logan visited the area in 1846 during early geological reconnaissance work. Decades later, Lawson recognized that these were sills, rather than basaltic flows, and named them after Logan (Lawson, 1893).

The present research, therefore, aims to resolve some of the key questions on the timing of major magmatic pulses and, particularly, the ages of mineralized intrusions, thus allowing a more refined picture of the complex and evolving magmatic plumbing system of the rift. Resolving some of these key timing questions will set the stage for more detailed questions such as why some intrusions are mineralized whereas others are not, the spatial and temporal variation of their potential mantle sources and variable metal fertility, and what parts of the volcanic sequence the intrusions may have fed. We here present new U-Pb ages on ~10 key units and discuss their implications. In an accompanying contribution (Smith et al., 2020), we focus in more detail on one mineralized intrusion, the Crystal Lake Intrusion southwest of Thunder Bay.

SCOPE OF THE PROBLEM: KEY EXAMPLES

Here we introduce the scope of the problem by highlighting two key magmatic units on the northern flank of the MCR, the Logan Sills near Thunder Bay and the Inspiration sill of the northern Nipigon Embayment (Fig. 1, Table 1). The iconic "Logan Sills" (Fig. 2)—so named by Lawson (1893) after the founder and first director of the Geological Survey of Canada—represent extensive and voluminous sill complexes on the north shore of Lake Superior. Early U-Pb dating studies suggested an age of 1109 +4/-2 Ma[2]. (Davis and Sutcliffe, 1985), on samples from the Lake Nipigon area. Since then, subtle geochemical differences in incompatible element ratios have suggested that sills in the Nipigon area (now called "Nipigon Sills") and sills in the Thunder Bay area (now "Logan Sills", *sensu stricto*) may actually form two distinct sill complexes (Hollings et al., 2007, 2010). A tentative age of 1114.7 ± 1.1 Ma was determined from a Logan Sill on Mount McKay, using a limited selection of very small baddeleyite grains (Heaman et al., 2007). This and other older age "outliers", such as the suggested age for the Inspiration sill of 1159 ± 33 Ma (Heaman et al., 2007), raised the possibility of an older and drawn-out start of MCR mafic magmatism, a finding that is at odds with modern dating studies on many large igneous provinces. With better and more robust high-precision U-Pb data, these studies typically show a sharp onset of high-volume mafic magmatism, on a time scale of 1 to 2 Myr, sometimes followed by additional pulses of diminishing volume and/or more varied composition over a 5 to 25 Myr time scale.

To help settle this important question of "the age of onset of voluminous mafic magmatism", we resampled both the Mt. McKay sill overlooking Thunder Bay and the Inspiration sill in the Nipigon area. In the field, we spent time collecting the most optimum samples of late-stage, more fractionated, and Zr-enriched pegmatoidal gabbros towards the top of both sills. Both samples returned adequate baddeleyite and some magmatic zircons (Fig. 3). Although at this stage all our results should be treated as preliminary, our data indicate improved ages for these sills at 1106.3 ± 2.0 Ma for the main Logan Sill capping Mt. McKay, and 1105.5 ± 3.0 Ma for the Inspiration sill (Fig. 4), i.e. within uncertainty of each other and also the original Davis and Sutcliffe (1985) data, respectively; and, importantly, also within uncertainty of the oldest high-precision

[2] In a subsequent paper, the three collinear zircon fractions are regressed from the orign to an upper intercept age of 1108.2±0.9 Ma (*see* Davis and Green, 1997).

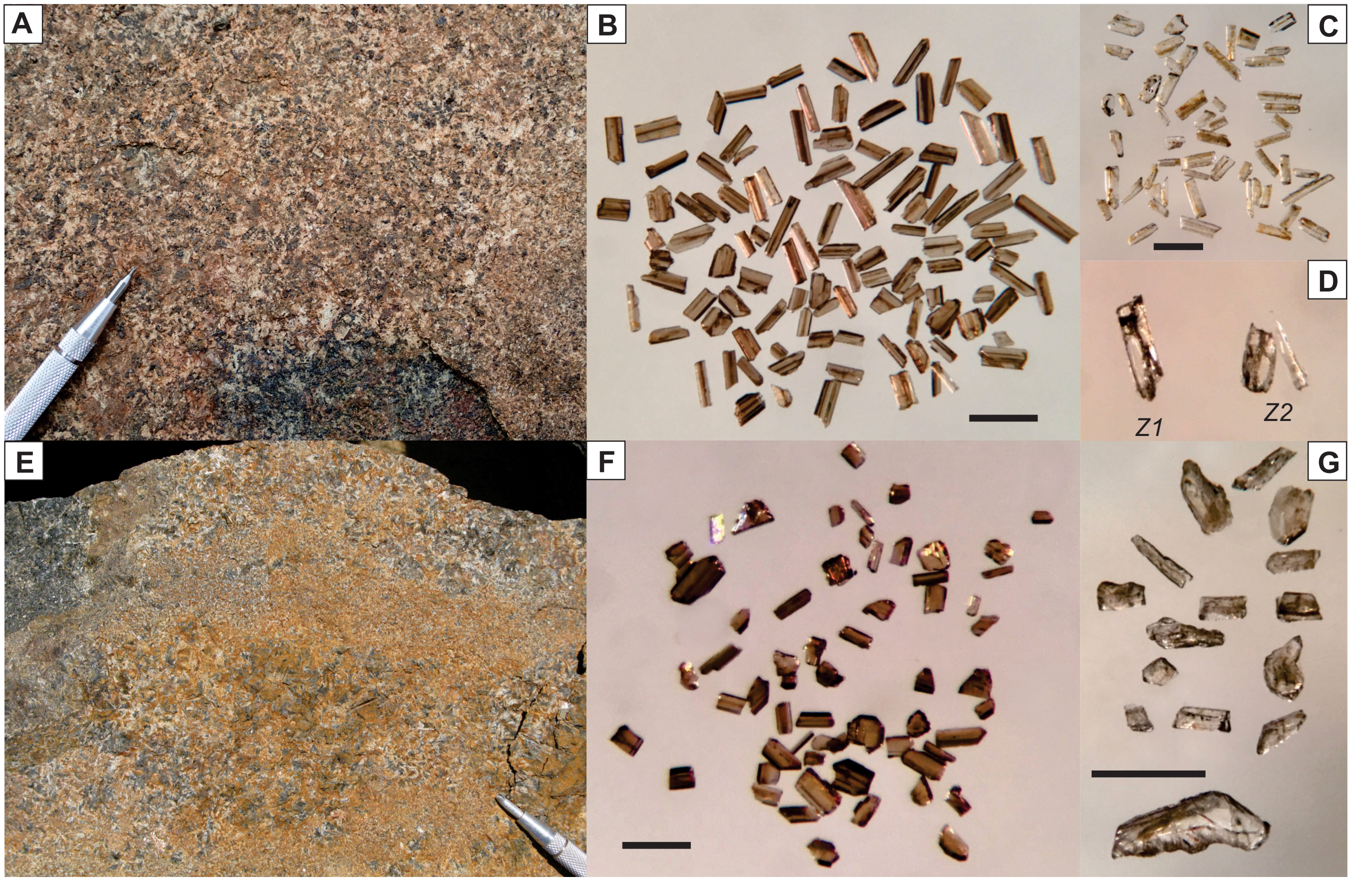

Figure 3. Typical baddeleyite and zircon recovery from pegmatitoidal gabbros near the top of Midcontinent Rift sills, the main Logan Sill at Mount McKay (a–d), and the Inspiration sill near Armstrong, Ontario (e-g). **a, e)** Photographs of sampled material, i.e. last-crystallizing differentiated pegmatoidal gabbro, which is typically underneath the chilled upper contact of the sills. **b, f)** Typical baddeleyite recovery. **c, d, g)** Blady late-stage magmatic zircons. All scale bars are 200 μm.

ages near the base of the volcanic successions around the rift at ca. 1107–1108 Ma (Davis and Sutcliffe, 1985; Davis and Green, 1997; Swanson-Hysell et al., 2019). These initial results confirm our intuition that the onset of the first high-volume mafic magmatism was indeed relatively sharply timed and occurred at ca. 1109–1107 Ma (*see also* Davis and Green, 1997), and that some of the more tentative results or interpretations on variably discordant small baddeleyite fractions from the Heaman et al. (2007) study were not quite accurate. Our results also demonstrate the remaining complexity, as few of the individual analyses are fully concordant. Although we recovered better baddeleyites than previous studies (Fig. 3), and also magmatic zircons in many cases, the blady magmatic zircon crystals in these types of samples do not withstand aggressive chemical abrasion and retain some discordance. If they are aggressively treated by chemical abrasion (Mattison, 2005), these crystals (Fig. 3c,d,g), with their cracks and accumulated damage, dissolve; with no or minimal chemical abrasion, they retain some discordance, requiring extrapolation to upper intercept ages. Nevertheless, these new improved ages represent a significant step forward.

In contrast to these improved, but nevertheless slightly discordant results on early high-volume diabase sill complexes, we here also discuss new zircon ages on well behaved gabbro samples from some of the mineralized intrusions, Tamarack in Minnesota and Crystal Lake in Ontario (Fig. 5). Both samples discussed here yielded abundant and relatively good quality zircons, which after chemical abrasion yielded fully concordant, overlapping data, and consequently highly precise and accurate ages on par with high-precision results on rhyolite samples in the volcanic successions. The sample from Tamarack, a differentiated pegmatoidal gabbro near the top of the "southern bowl" of this large composite intrusion, yielded a zircon concordia age (Ludwig, 1998, 2003) of 1103.8 ± 0.9 Ma based on three fully overlapping single zircon data (Fig. 5a). This age is clearly younger than the 1107–1109 Ma onset of high-volume mafic magmatism but could correlate with the nearby volcanic sequence of the "Chengwatana basalts" (Wirth and Gehrels, 1998) in the southwestern extension of the MCR (Fig. 1). A mineralized, pegmatoidal, vari-textured gabbro from the northern arm (or "limb") of the Crystal Lake Intrusion yields a fully concordant zircon and badde-

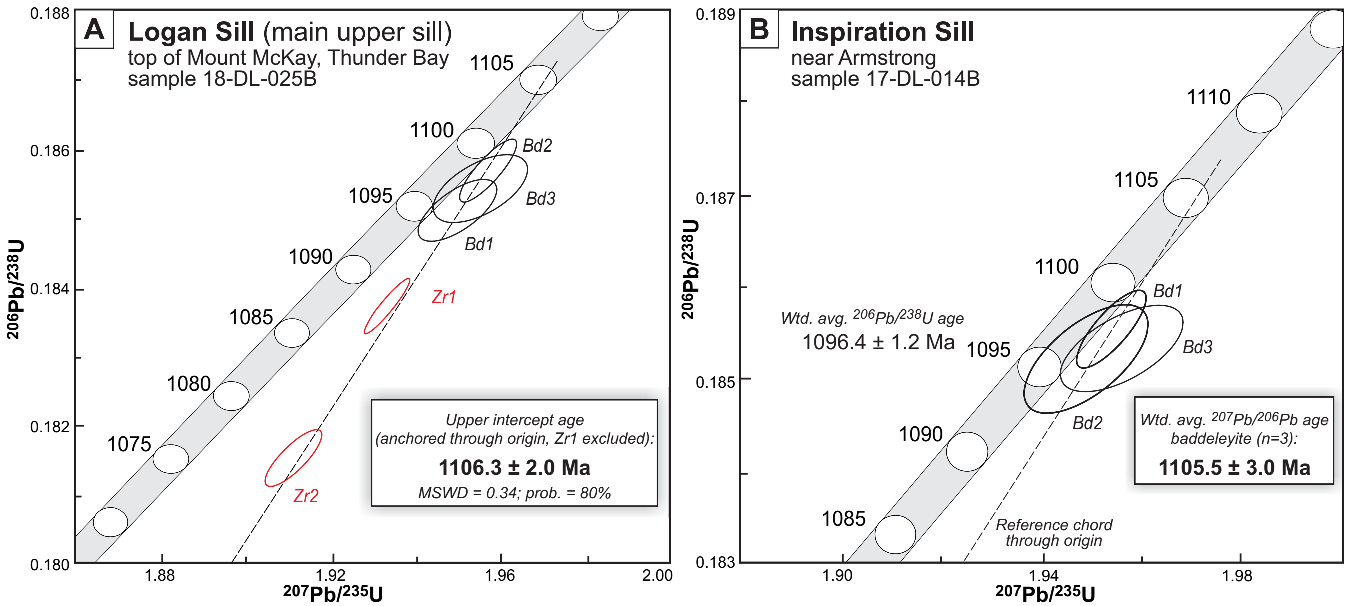

Figure 4. U-Pb concordia diagrams for **(a)** the Logan Sill at the top of Mt. McKay (sample 18-DL-025B) and **(b)** the Inspiration sill (sample 17-DL-014B) from the northern Nipigon Embayment. Zircon (Zr) data are shown as red ellipses and baddeleyite (Bd) as black ellipses. Preferred age picks are shown in bold font. All data-point error elipses are 2σ.

leyite age of 1093.2 ± 1.2 Ma (Fig. 5b), distinct and considerably younger than the 1099.6 ± 1.2 Ma date on discordant baddeleyite fractions reported by Heaman et al. (2007). This younger age suggests a correlation of the Crystal Lake Intrusion, not with the main Duluth Complex, but rather with the younger intrusions in the roof of that complex, such as the Beaver Bay Complex. Results on multiple samples from the Crystal Lake Intrusion and a more detailed interpretation is presented in Smith et al. (2020).

SAMPLING STRATEGY AND OVERVIEW OF RESULTS

Fieldwork over the last 2–3 years has allowed us to visit many of the key intrusive units, often with local experts. We have specifically targeted mineralized intrusions, and intrusions deemed of interest to exploration. We have also targeted representative units of some of the main magmatic pulses that were still lacking precise and accurate ages (e.g. Logan Sills), as well

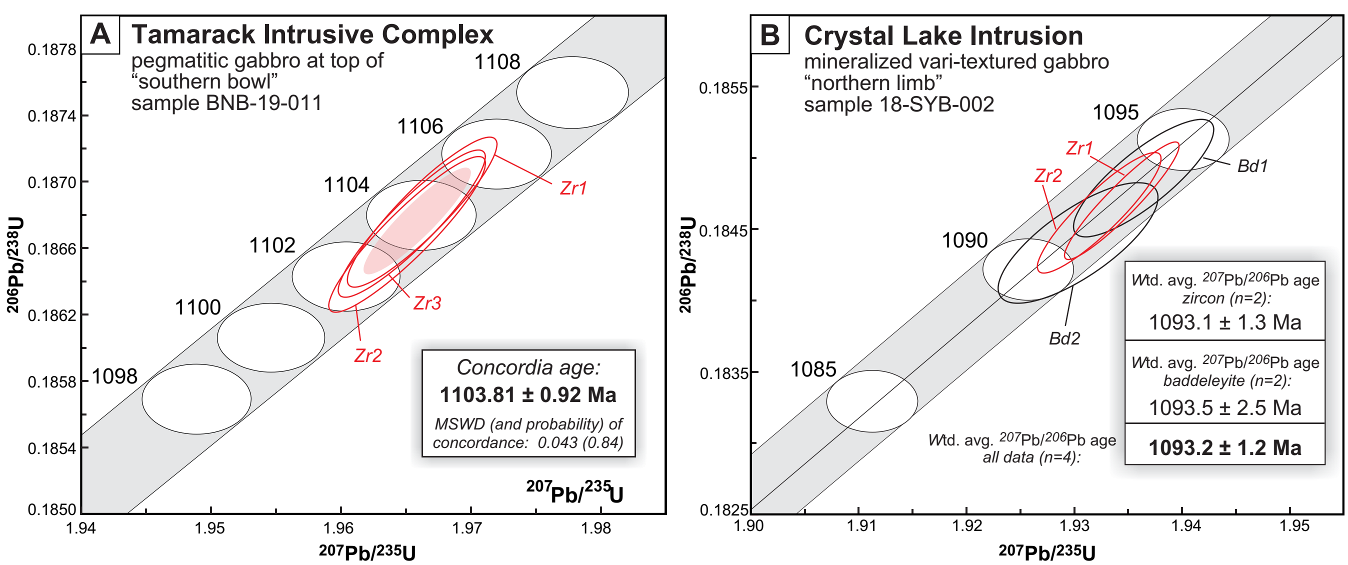

Figure 5. U-Pb concordia diagrams and preliminary ages for **(a)** the main "southern bowl" of the Tamarack Intrusion, Minnesota; and **(b)** the mineralized vari-textured gabbros from the northern limb of the Crystal Lake Intrusion. For the Tamarack sample, three fully concordant and overlapping zircon analyses define a concordia age (filled ellipse) of 1103.8 ± 0.9 Ma, distinctly younger than the earlier onset of high-volume basaltic magmatism in the Midcontinent Rift (at ca. 1106–1110 Ma). For Crystal Lake (b), we show one well behaved sample with concordant and overlapping zircon and baddeleyite results. Additional results are discussed in Smith et al. (2020). All data-point error elipses are 2σ.

as some of the problematic age “outliers” (e.g. Inspiration sill, and members of the Pigeon River dyke swarm). In all these cases, we spent time in the field to evaluate the overall complexity of the intrusions and their different phases, after which we sampled optimum material for U-Pb dating (~10 kg, sometimes multiple samples): typically coarser grained, slowly cooled, more fractionated units in which incompatible elements such as Zr (and U) show elevated abundances, thus increasing the likelihood that larger and more abundant baddeleyite and/or zircon crystals would have crystallized. In some of the composite or multi-phase intrusions, we sampled more than one phase, including both the presumed oldest and youngest phases—although the general expectation is that all of these will be within the resolution of the typical data, ideally ~1 Myr[3].

At the same time, we have compiled and evaluated all previous work (Table 1), feeding into our overall prioritization of samples. Needless to say, the requirement for accurate high-precision ages keeps increasing, as models are improving and associated questions are refined. Hence, this work is never finished and a number of samples are still in progress. Nevertheless, we can present here ~10 new ages for key units around the MCR, including some of the mineralized intrusions on the Canadian side of the border (Table 2). All results should be treated as preliminary, as additional fractions are still being analyzed. For analytical methods, the reader is referred to the accompanying paper by Smith et al. (2020, *see* their Appendix 1).

MINERALIZED INTRUSIVE COMPLEXES OF THE MIDCONTINENT RIFT: SOME KEY EXAMPLES

Sunday Lake Intrusion

The recently discovered Sunday Lake Intrusion, located in Jacques Township, ~25 km north of Thunder Bay, intrudes Archean metasedimentary rocks and granitoids of the Quetico Subprovince (Fig. 6). The intrusion, now dated at 1109.0 ± 1.3 Ma (this study; Table 2), is emplaced along the Crock Lake Fault, interpreted as a splay of the main Quetico Fault to the north (Flank, 2017), and is characterized by a distinct, elliptical, reversely magnetized anomaly. The morphology and true extent of the intrusion is yet to be fully determined; however, drilling indicates that the body is tabular in shape where emplaced into Quetico metasedimentary rocks, and more tube-like (cylindrical) to the northwest where it is hosted by Archean granitoids (Fig. 6). The differentiated intrusion is divided into an Ultramafic Series, a Lower Gabbro Series, and an Upper Gabbro Series (Flank, 2017) on the basis of petrographic and geochemical characteristics. The 10–120 m thick basal Ultramafic Series is composed of gabbroic breccia, melagabbro, olivine melagabbro, peridotite, and minor pyroxenite. The 250 m thick Lower Gabbro Series consists of gabbro, melagabbro, and peridotite. The evolved, coarse-grained Upper Gabbro Series is comprised of strongly hematized leucogabbro, oxide-rich gabbro, and evolved monzogabbro. The upper contact is commonly brecciated, containing subangular and partially resorbed quartz fragments and Quetico metasedimentary xenoliths within a chilled, hematized groundmass.

Sulphide mineralization within the Sunday Lake Intrusion is disseminated (2–10 vol.%) and mainly concentrated along the basal contact of the Ultramafic Series. The main mineralized body, which is enriched in Cu, Pt, Pd, and Au at typical levels of 3–10 g/t Pt+Pd+Au, contains disseminated, high PGE-tenor sulphides composed of chalcopyrite, pyrite, and pyrrhotite. Drilling has indicated that the main orebody can be traced over a 1500 x 900 m area, with a thickness of up to 43 m (Flank, 2017; S. Flank, pers. comm., 2019). Lower grade (<1 ppm Pt+Pd+Au), high-tenor sulphide mineralization (≥1200 ppm Pt+Pd+Au in 100% sulphide) has also been recognized within laterally continuous horizons at the upper and lower contacts of the Lower Gabbro Series (Flank, 2017). Footwall stringers, enriched in Cu and PGEs have also been noted.

Current Lake Intrusive Complex

The Thunder Bay North Igneous Complex, located ~50 km northeast of Thunder Bay, comprises a series of small, mineralized ultramafic-mafic intrusions that have been emplaced in proximity to the east-west-trending Quetico Fault, and are hosted within the Archean Quetico Subprovince (Fig. 7). Intrusions of the Thunder Bay North complex, which include the Current Lake, Steepledge, and Lone Island Lake intrusive complexes and possibly other bodies, are associated with the early stages of the MCR development and are prospective targets for Pt-Pd-Cu-Ni sulphide mineralization. The Current Lake Intrusive Complex, which we have dated at 1106.6 ± 1.6 Ma (this study; Table 2), is a tubular to tabular conduit-like deposit that is characterized by a “tadpole”-shaped aeromagnetic anomaly that extends for ~6 km in a northwest-southeast direction and widens to the southeast (Fig. 7a; Goodgame et al., 2010; Thomas et al., 2011). The Current Lake Complex, along with the adjacent paral-

[3] Most magmatic complexes are emplaced within the time span of a typical magmatic pulse of less than 1 Myr. Resolving complexity on shorter time scales, in Proterozoic rocks, remains very challenging. An interesting example is the study by Mungall et al. (2016) of the Bushveld Complex, although this study remains controversial.

Table 2. Summary of precise and robust U-Pb ages for key intrusions, including new results from the present study (results in bold font). The data are organized into two groups: intrusions on the northern flank of the Midcontinent Rift versus those on the southern flank. The age for the Kitto mafic-ultramafic intrusion is shown in red, as it remains one of the significant older age "outliers" for the onset of high-volume mafic magmatism still to be tested. Work on this sample is in progress. Intrusions known to have mineralization are preceded by an asterisk (*).

Rock Unit	New U-Pb Age (Ma)[1]	Method[2]	References	Sample ID	Easting (mE)	Northing (mN)	Zone	Description
Precisely dated intrusions on northern flank of MCR:								
* Kitto mafic-ultramafic intrusion	1117.4±3.7	Bd, wm7/6, n=2	Heaman et al., 2007					
* Seagull intrusion	1112.8±1.4	Bd, complex results	Heaman et al., 2007					
* Jackfish intrusion	1112.4±2.8	Bd, wm6/8, n=2	Heaman et al., 2007					
* Disraeli intrusion	1109.9±1.5	Bd, wm7/6, n=2	Heaman et al., 2007					
Cloud R. dyke	**1109.2±2.9**	**Bd, u. intercept, n=3**	**This study; *see also* Heaman et al., 2007**	**BNB-19-023**	**313140**	**5329177**	**16U**	**Main NNW-trending dykes, at Crooks; is cut by Pigeon River dykes**
* **Sunday Lk intrusion**	**1109.0±1.3**	**Bd, wm, n=5, slightly disc.**	**This study**	**BNB-17-050D**	**334842**	**5394958**	**16U**	**Sunday Lake Intrusion, coarser red monzogabbro; DDH SL-15-013, 481.0-485.4 m**
* Thunder Intrusion	1108.0±1.0	Zr, wm7/6, n=3, conc.	Trevisan et al., 2015					
* Coldwell Complex	1108.0±1.0	Zr, u. intercept	Heaman and Machado, 1992					
Nipigon Sills	1108.2±0.9	Zr, u. intercept, n=3	Davis and Sutcliffe, 1985; *see* Davis and Green, 1997					Diabase, pegmatitic gabbro, granophyre; these sills were referred to as "Logan Sills" by Davis and Sutcliffe, 1985; more precise upper intercept is quoted in Davis and Green, 1997.
Swamper Lk monzogabbro	1107.0±1.1	Zr, wm7/6, n=3	Davis and Green, 1997					Monzogabbro, reversely magnetized; age suggest link with Logan Sills
* Hele intrusion	1106.6±1.5	Bd, wm7/6, n=2	Heaman et al., 2007					
* **Current Lake Complex**	**1106.6±1.6**	**Zr and bd, u. intercept, n=4**	**This study**	**18-DL-035**			**16U**	**Coarser red monzogabbro near top of intrusion, Beaver Lake part of intrusive complex**
Logan Sills	**1106.3±2.0**	**Zr and bd, u. intercept, n=4**	**This study**	**18-DL-025B**	**330558**	**5357158**	**16U**	**Coarse-grained diabase, with incipient pegmatoidal segregations below uppper contact of upper sill**
Kama Hill sill	**1106.3±3.6**	**Zr, u. intercept, n=4**	**This study**	**BNB-19-024A**	**428116**	**5424370**	**16U**	**Coarse-grained to pegmatoidal diabase below upper contact of main sill**
Inspiration sill	**1105.5±3.0**	**Bd, wm7/6, n=3**	**This study**	**17-DL-014B**	**356197**	**5573323**	**16U**	**Pegmatoidal segregations in upper part of diabase sill**
* Nemegosenda	1105.4±2.6	Zr, u. intercept, n=3	Heaman et al., 2007					
* Tamarack Intr. Complex northern body "CGO"	1105.6±1.3	Bd, wm, n=3, slightly disc.	Goldner, 2011				15T	Feldspathic lherzolite from near margin of northern dyke-like body ("CGO")
* **Tamarack Intr. Complex northern body "CGO"**	**1105.9±0.9**	**Zr, u. intercept, n=4**	**This study**	**BNB-19-015**	**492042**	**5170155**	**15T**	**Pegmatoidal gabbro from upper part of northern dyke-like body ("CGO") DDH 15-TK-0221, 440.00–463.00 m: coarse-grained to pegmatoidal gabbro**
* **Tamarack Intr. Complex central body "FGO"**	**1103.7±0.8** **1105.7±0.8**	**Zr, conc. age, n=4** **Zr, wm7/6, n=4**	**This study**	**BNB-19-013** **BNB-19-014**	**492042**	**5170155**	**15T**	**Pegmatoidal gabbro from upper part of central dyke-like body ("FGO"), DDH 15-TK-0218, 503.46–510.30 m** **Late crosscutting dyke of quartz dioritic pegmatoid, cutting FGO peridotite, DDH 15-TK-0218, 1059.55–1063.30 m**
* **Tamarack Intr. Complex southern bowl ("Bowl")**	**1103.8±0.9**	**Zr, conc. age, n=3**	**This study**	**BNB-19-011**	**496841**	**5163275**	**15T**	**Pegmatoidal gabbro from upper part of main southern part of intrusion ("the bowl") DDH 15-TK-0217, 193.60–199.80 m: coarse-grained to pegmatoidal gabbro**
* Duluth Complex	1099.0±1.0	Zr, wm7/6, several results	Paces and Miller, 1993					
Mt. Josephine dyke	**1099.0±1.2**	**Zr and bd, wm7/6, n=4**	**This study**	**18-DL-022**	**301962**	**5316973**	**16T**	**Coarse-grained, in part pegmatoidal, diabase from middle of ~100 m wide dyke**
Pigeon R. dykes	**1096.9±1.9**	**Zr, u. intercept, n=3**	**This study**	**17-DL-004B**	**310563**	**5324695**	**16U**	**Rita Bolduc dyke (~80–100 m), one of the main NNE-trending Pigeon River dykes**
Mount Mollie dyke	**1096.3±1.4**	**Zr and bd, u. intercept, n=6**	**Smith et al., 2020**					
* Sonju Lake Intrusion	1096.1±0.8	Bd, wm7/6, n=4	Paces and Miller, 1993					
* Beaver Bay Complex	1095.8±1.2	Zr and Bd, wm7/6, n=6	Paces and Miller, 1993					Beaver River Diabase complex
Hovland Sill	1095.9±0.6	Zr, wm6/8, concordant	Boerboom et al., 2014					
* **Crystal Lake Intrusion vari-text. gabbro, S limb**	**1094.1±1.4**	**Zr and bd, wm7/6, n=4**	**Smith et al., 2020**	**18-SYB-111**	**306239**	**5326523**		**Vari-textured gabbro, southern limb, minor sulphides and Cr-spinel; DDH CL0003, 556–562 m**
* **Crystal Lake Intrusion vari-text. gabbro, N limb**	**1093.1±1.2**	**Zr and bd, wm7/6, n=4**	**Smith et al., 2020; summarized in this paper**	**18-SYB-002**	**305453**	**5328330**		**Vari-textured gabbro, northern limb, minor sulphides and Cr-spinel; DDH CL0001, 412–417 m**
* **Crystal Lake Intrusion combined data**	**1092.3±0.7**	**Zr and bd, conc. age, n=6**	**Smith et al., 2020**	**18-SYB-001, 002, 111**				
* **Crystal Lake Intrusion Troctolite, unmineralized, N limb**	**1091.4±1.4**	**Zr, wm, n=2**	**Smith et al., 2020**	**18-SYB-001**	**305453**	**5328330**		**Homogeneous medium- to coarse-grained troctolite**
Moss Lake Gabbro	1094.7±3.1	Bd, wm6/8, n=2	Heaman et al., 2007					Intrusive complex emplaced within Osler Group, on Black Bay Peninsula
St. Ignace Isl. Complex	1089.2±3.2	Zr, no details available	Smyk et al., 2006					Intrusive complex emplaced within Osler Group
Precisely dated intrusions on southern flank of MCR:								
* Echo Lake Intrusion	1111.0±1.0	Zr, overlapping conc.	Canon and Nicholson, 2001; S. Nicholson, pers. comm., 2018					Large gabbroic layered intrusion with basal ultramafic units; buried
* Eagle - Eagle East complex	1107.3±3.7	Bd, wm7/6, n=4	Ding et al., 2010					Peridotite and gabbros, in feeder-like dykes
* **Bovine Igneous Complex**	**1106.2±1.3**	**Bd, wm, n=3, slighltly disc.**	**This study**	**18-DL-001**	**396985**	**5174336**	**16T**	**Coarse gabbro, from outcrop along southeastern rim of intrusion**
* Mellen Complex	1102.8±2.8	Zr, u. intercept.	Zartman et al., 1997					Layered intrusion with mafic lower part and granitic upper part

Notes and abbreviations: bd = baddeleyite, conc. = concordant, DDH = diamond drillhole, disc. = discordant, Gp = Group, Lk = Lake, Mt = Mount, n=x = number of analyses, R = River, u. intercept = upper intercept, wm = weighted mean, zr = zircon.

1: Ages in bold font are new ages obtained as part of the present study. The Kitto age of Heaman et al. (20017) is one of the remaining age "outliers" and shown in red font.

2: CA-ID-TIMS on single zircons or small fragments thereof, unless otherwise noted; baddeleyite untreated.

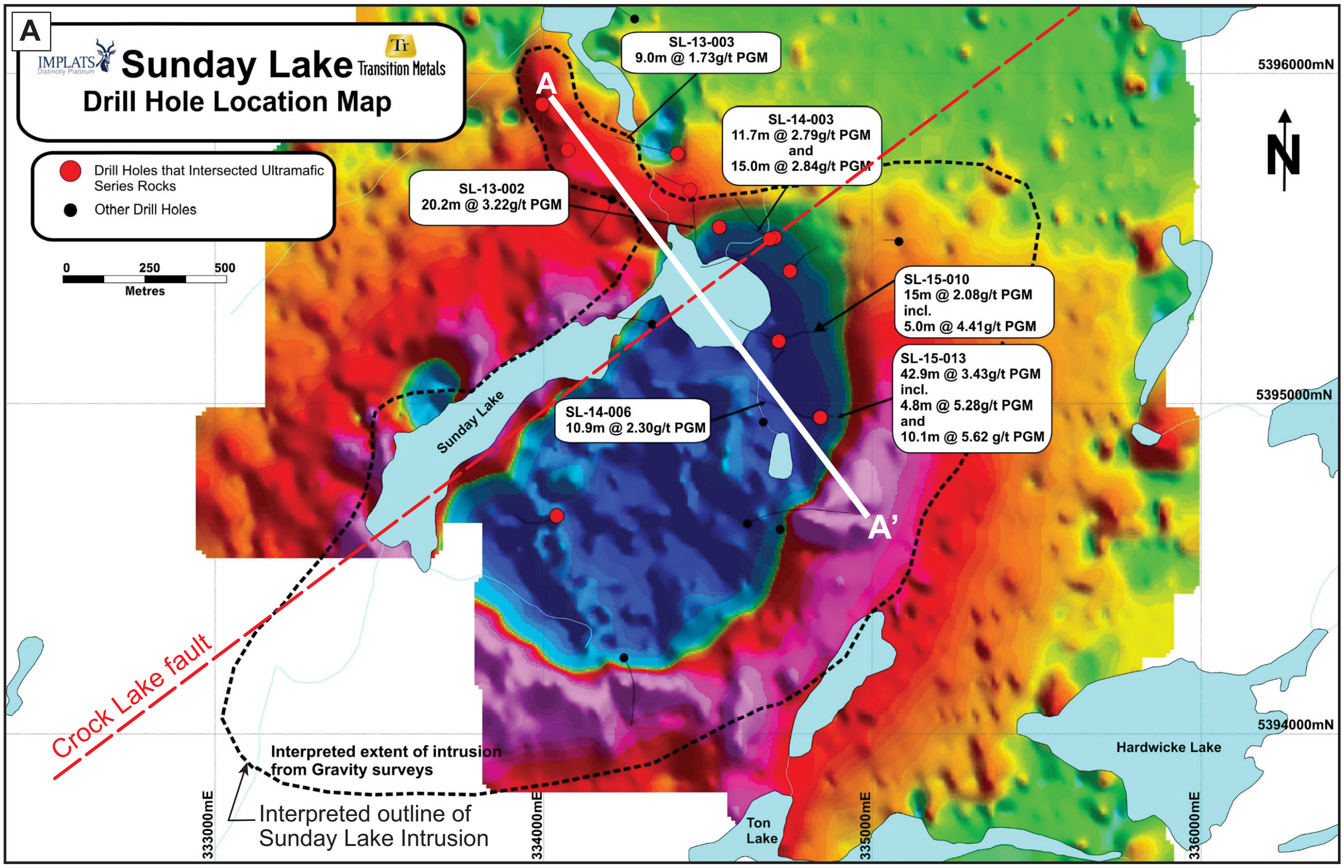

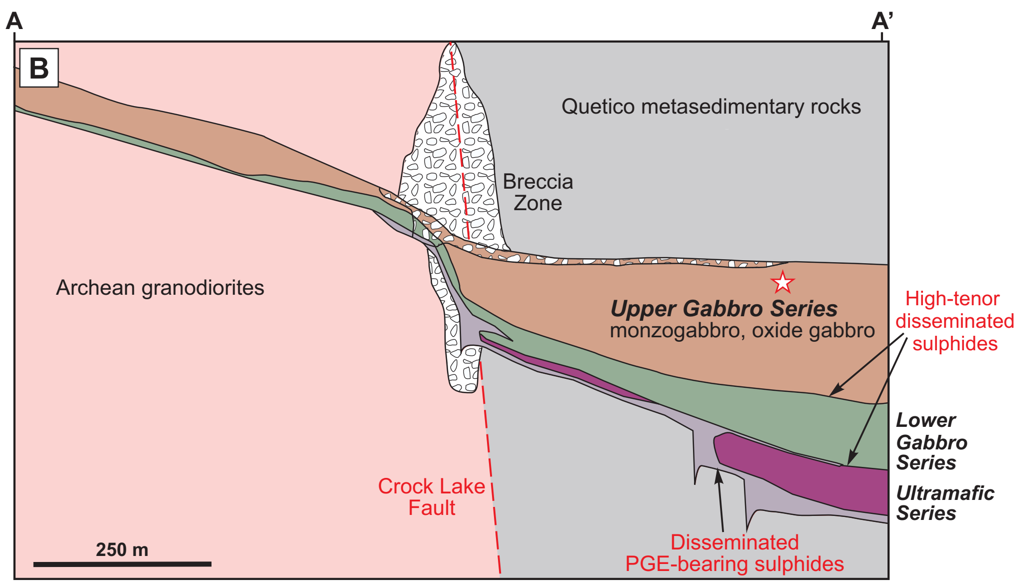

Figure 6. Summary figure of the Sunday Lake Intrusion (courtesy Steve Flank and North American Palladium): **a)** Airborne magnetic map with the inferred outline of the intrusion; **b)** Section A-A'. The dated sample is from the upper monzogabbro unit, in DDH SL-15-013 (schematically indicated with the red star).

lel Steepledge Complex, shows variation in shape, composition, orientation, and grade along its length. The change in morphology of the Current Lake Intrusive Complex from tubular to more tabular coincides with the contact between Archean granitoids in the north and Quetico metasedimentary rocks in the south. Pre-existing structures in the Quetico Subprovince are also thought to have strongly controlled the initial emplacement of the Thunder Bay North magmas.

Extensive drilling has delineated a 3.4 km long, continuously mineralized, disseminated sulphide body that is hosted within the ultramafic portion of the complex and is characterized by Pt/Pd ratios of >1 and Ni/Cu ratios of ~0.5 (Goodgame et al., 2010; Thomas et al., 2011). In the north, the Current Lake Intrusive Complex is a subhorizontal, sinuous, tubular body composed mainly of olivine melagabbro and lherzolite, ranging from ≥30 m in diameter, up to 50 m in width and 70 m in thickness (Goodgame et al., 2010;

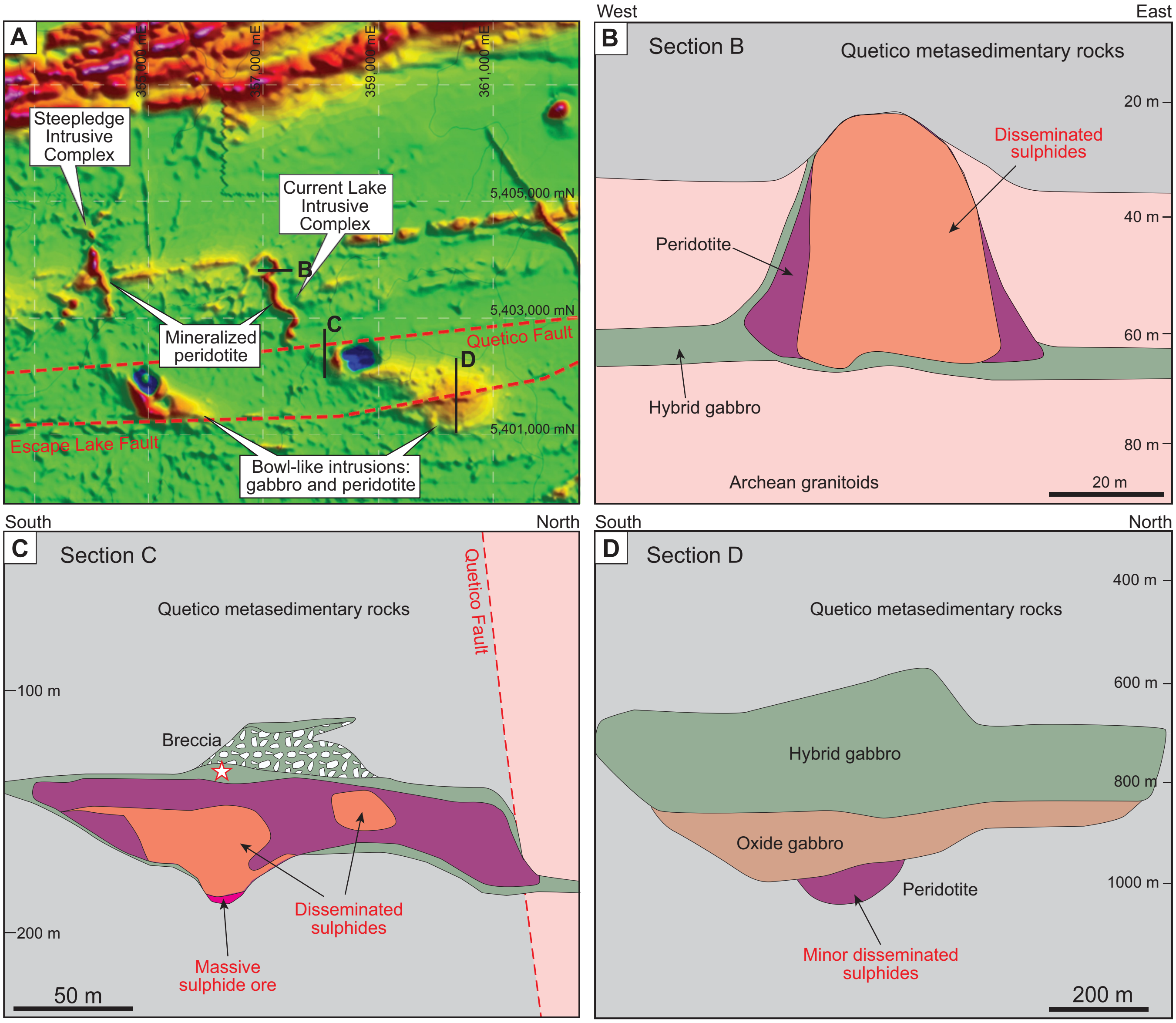

Figure 7. Summary figures of the Thunder Bay North Complex and its Current Lake Intrusive Complex. **a)** Summary magnetic map (total intensity) showing the various parts of the Current Lake complex (image courtesy of Allan MacTavish, Panoramic Resources, and pers. comm., 2018). The map highlights the NNW-SSE-trending "tadpole"-shape anomalies of the Current Lake and Steepledge Lake intrusive complexes. The locations of the cross-sections shown in figures (b) to (d) are also shown. **b)** Cross-section through the northern part of the Current Lake complex (looking north); in this section, the intrusion is tube-like in morphology with mineralization disseminated throughout the interior of the chonolith. **c)** Cross-section (looking east) through the Beaver Lake portion of the Current Lake Intrusive Complex. **d)** Cross-section (looking west) through the South-East anomaly. Cross-sections from Thomas et al. (2011) and A. MacTavish (Panoramic Resources, pers. comm., 2018). Approximate location of our dated sample shown by a red star.

Thomas et al., 2011). Here Pt-Pd-Cu-Ni sulphide mineralization is disseminated in nature and distributed throughout the entire tubular body (Fig. 7b). To the southeast, the peridotite intrusion progressively deepens and becomes a shallowly plunging tabular body in the Beaver Lake area, with dimensions up to 600 m wide and 200 m thick (Goodgame et al., 2010; Thomas et al., 2011). Sulphide mineralization is more localized in this area and is confined to the margins of the conduit. Semi-massive to massive sulphides have been locally intersected here, along the basal contact of the intrusion (Fig. 7c). Near the top of the intrusion, a different style of mineralization has been identified, characterized by finely disseminated, high-tenor Cu-bearing sulphides (Goodgame et al., 2010). The southeastern extent of the Current Lake Complex, defined by a circular magnetic anomaly, is represented by the differentiated, tabular, unmineralized "Southeast Anomaly", which is composed of a basal peridotite, overlain by an oxide gabbro, and a distinctive red, hybrid gabbro that is strongly hematized and contaminated.

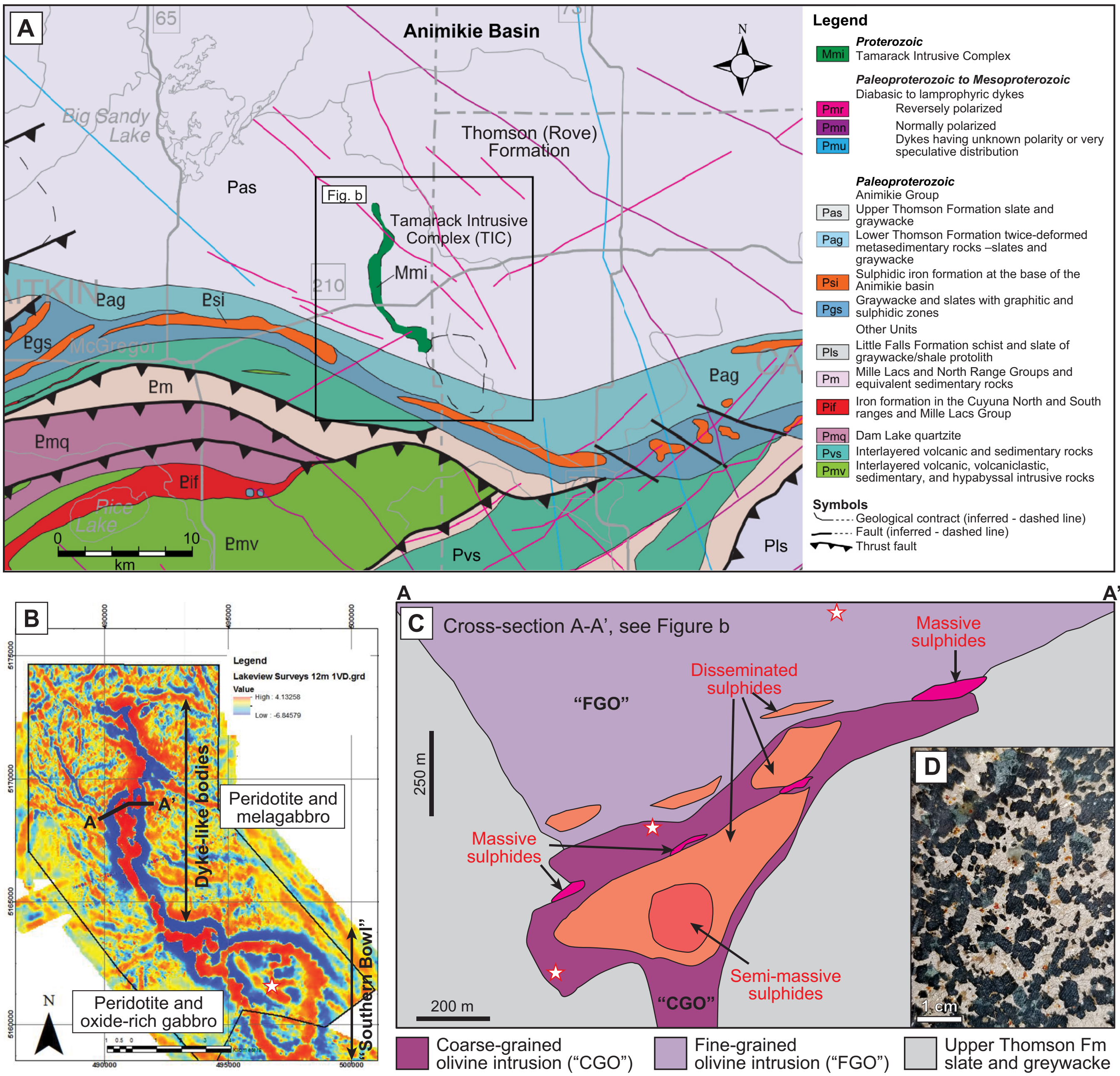

Figure 8. Summary figures of the Tamarack Intrusive Complex. **a)** Regional geological setting and location of the Tamarack complex, which intrudes slate and greywacke of the Rove Formation in the southern Animiki Basin (*from* the geological map of Minnesota; Jirsa et al., 2011). **b)** Airborne magnetic map image (1st vertical derivative) showing the overall shape of the Tamarack Intrusive Complex, with the northern dyke-like bodies and the "southern bowl". **c)** West-to-east cross-section A-A' (*see* Fig. (b) for location), showing the coarse-grained olivine ("CGO") and fine-grained olivine ("FGO") intrusions within the northern dyke-like part of the Tamarack Intrusive Complex (*after* Taranovic et al., 2015). **d)** Net-textured to semi-massive sulphide ore in drill core from the CGO intrusion.

Tamarack Intrusive Complex

The mafic-ultramafic Tamarack Intrusive Complex, located ~75 km to the southwest of the Duluth Complex, intrudes Paleoproterozoic slate and greywacke of the Upper Thomson Formation within the Paleoproterozoic Animikie Basin (Fig. 8). The complex is characterized by a tadpole-shaped aeromagnetic anomaly, which extends ~13 km in a northwest-southeast direction and varies from 1 to 4 km in width (Fig. 8; Goldner, 2011; Taranovic et al., 2015). The complex, interpreted as a dynamic open-system conduit that crystallized from a picritic parental magma (Taranovic et al., 2015), consists of three sub-intrusions: the "coarse-grained olivine" (CGO), the "fine-grained olivine" (FGO), and the southern "bowl" intrusions. The mineralized CGO and FGO intrusions are located in the north, where they form the dyke-like portion of the Tamarack Intrusive Complex, with an overall morphology of an irregular funnel (Fig. 8c). The 1105 ± 1.2 Ma CGO intrusion (Goldner, 2011), which comprises the lower portion of the funnel-like dyke, is composed of coarse-grained peridotite, feldspathic peridotite, melatroctolite, and melagabbro (Taranovic et al., 2015). The overlying FGO intrusion is characterized by fine-grained peridotite, feldspathic peridotite, feldspathic pyroxenite, and melagabbro (Taranovic et al., 2015). The "bowl" intrusion, which appears barren of sulphide mineralization, is composed of peridotite and feldspathic peridotite overlain by a differentiated sequence of oxide-rich gabbronorites (Goldner, 2011). At present, uncertainty surrounds the relative timing of the three intrusions. Our new zircon concordia age of 1103.8 ± 0.9 Ma, based on three fully overlapping single zircon results (Fig. 5a), was obtained on pegmatoidal gabbro near the differentiated top of the southern bowl.

The Ni-Cu-PGE sulphide mineralization within the Tamarack Intrusive Complex (Fig. 8c) is hosted within the CGO and FGO intrusions and includes minor massive, disseminated, and net-textured sulphide ores characterized by Ni/Cu ratios of >1 (Taranovic et al., 2016). Current inferred resource estimates indicate 4.3 Mt at 1.58% Ni, 0.92% Cu, 0.29 g/t Pt, and 0.18 g/t Pd (Fletcher et al., 2018). The CGO intrusion hosts the majority of the mineralization as disseminated and semi-massive (net-textured) sulphides, which are typically localized within the core of the dyke. The FGO intrusion hosts disseminated and patchy net-textured sulphide mineralization that is confined to discrete layers near the base of the intrusion, above the FGO-CGO contact. Massive sulphide lenses are found at the contact between the FGO-CGO intrusions and in adjacent country rocks (Fig. 8c). The sulphide ores are characterized by variable proportions of the primary magmatic assemblage pyrrhotite, pentlandite, chalcopyrite, and magnetite, with accessory pyrite and cubanite (Taranovic et al., 2016). Platinum group element tenors are variable throughout the Tamarack Intrusive Complex ores (Taranovic et al., 2016), a feature attributed to variable R-factors. The highest PGE tenors, which are comparable to those of Noril'sk ores, are associated with disseminated ores of the CGO intrusion. It has been suggested that the high-tenor sulphides of the CGO intrusion formed as a result of upgrading of an earlier sulphide liquid, left in the conduit system by the inferred earlier FGO magma (Taranovic et al., 2016). Although crustal contamination is thought to have played a critical role in ore genesis and in attaining S saturation, this is not recognized within the preserved isotopic record. Sulphides within the Tamarack Intrusive Complex are characterized by mantle-like $\delta^{34}S$ values between -0.2 and 2.8‰ (Taranovic et al., 2018), which are in sharp contrast with those from the basal disseminated ores of the Duluth Complex ($\delta^{34}S$ 0–18‰; Ripley et al., 2007; Queffurus and Barnes, 2014). Furthermore, O and Re-Os isotope compositions indicate only low degrees of contamination (<3%). Taranovic et al. (2018) suggest that the isotopic characteristics of the Tamarack Intrusive Complex could be a function of either selective contamination of Paleoproterozoic sedimentary rocks or efficient isotopic exchange within the dynamic conduit system. If exchange reactions have operated to obliterate the initial isotopic signature, then such isotopes are no longer accurate proxies for estimating crustal contamination.

Eagle and Eagle East Intrusions

Prior to the discovery of extensive, high-grade, massive Ni-Cu sulphides at the Eagle intrusion in 2002, Ni-Cu-PGE mineralization in the MCR was thought to be hosted by larger, sheet-like mafic intrusions (e.g. Duluth Complex, Crystal Lake). The Eagle discovery changed this perspective, resulting in a wave of exploration for magmatic sulphide deposits focussed on smaller, early rift, conduit-type intrusions.

The small ultramafic Eagle intrusion and nearby Eagle East intrusion intrude Paleoproterozoic rocks of the Marquette Range Supergroup within the Baraga Basin, which is also host to the MCR east-west-trending Marquette-Baraga dyke swam (Fig. 9). The Eagle and Eagle East intrusions (formerly known as the Yellow Dog Peridotites; Morris, 1977), are characterized by prominent ellipse-shaped magnetic highs (long-axis parallel to the dyke swarm) and occur as separate subvertical, boat-shaped, dyke-like bodies (Fig. 9; Ding et al., 2010; Barnes et al., 2016). Barnes et al. (2016) suggest the morphology of these intrusions resulted from conduit widening of an initial blade-shaped dyke (cf. Savannah, Western Australia). The Eagle intrusion is 480 m long and 100–200 m wide, with a vertical extension of >300 m. The deeper Eagle East intrusion is ~600 m long, ~150 m wide, and >500 m thick (Ding et al., 2010). Both are emplaced above the unconformity with the Archean basement.

The Eagle and Eagle East intrusions contain significant Ni-Cu-PGE mineralization, with current estimates indicating a combined resource of 4.8 Mt at 2.8% Ni, 2.4% Cu, 0.7 g/t Pt, and 0.5 g/t Pd (Clow et al., 2017). The sulphide mineralization is characterized by disseminated, semi-massive and massive sulphide ores, which are composed of pyrrhotite, pentlandite, chalcopyrite, and cubanite (Ding et al., 2010, 2012). At Eagle, over 90% of the sulphide ore occurs in the irregular-shaped massive sulphide zone above the keel of the intrusion, with some ore also hosted within adjacent metasedimentary rocks (Fig. 9c,d). At Eagle East, high-grade semi-massive and massive sulphide ores are confined

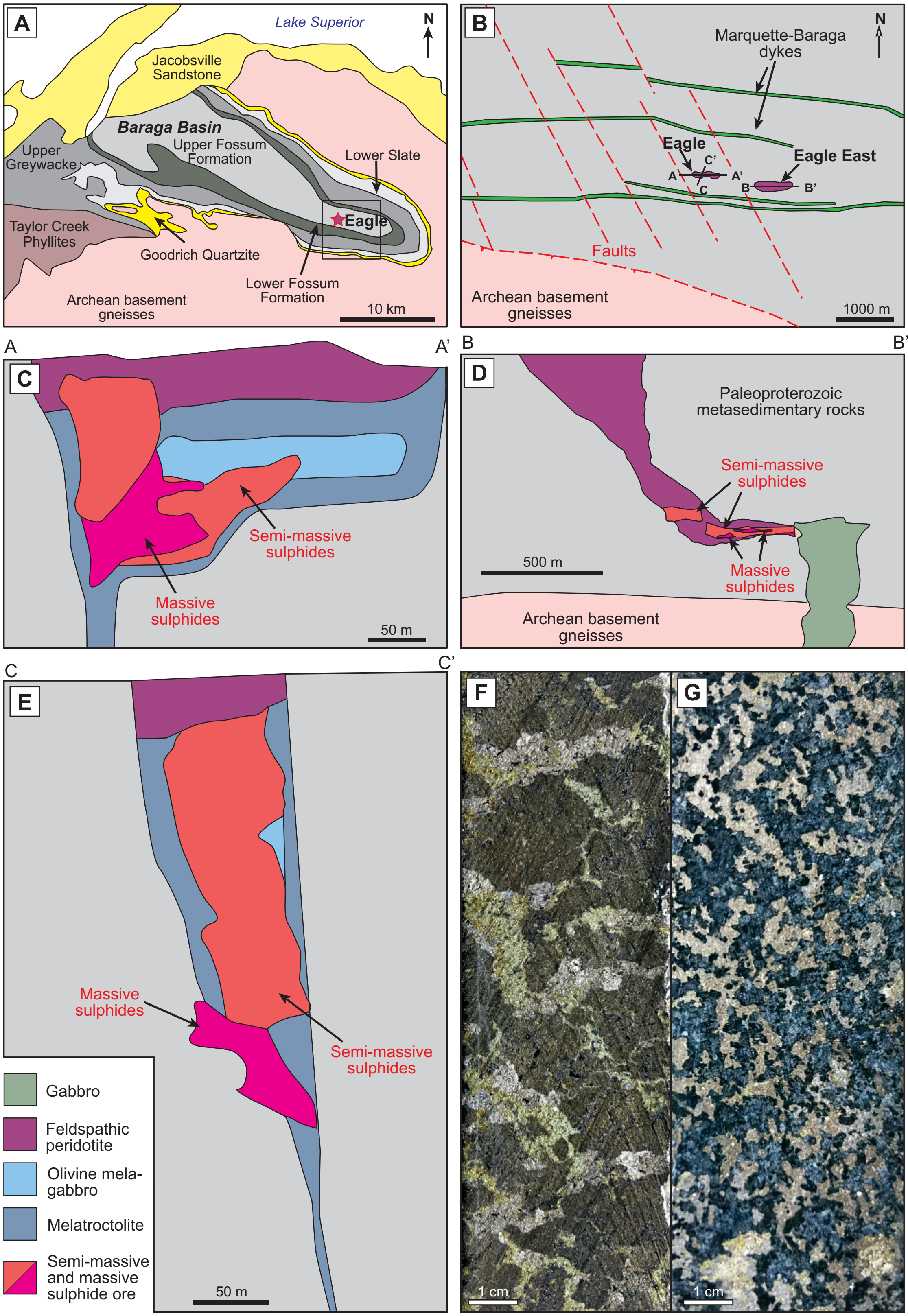

Figure 9. a) Geological setting of the Eagle deposit in the synclinorium of the Paleoproterozoic Baraga Basin (*after* Ding et al., 2010). **b)** Plan view of the Eagle and Eagle East intrusions in the eastern Baraga Basin. The intrusions are elongated in an east-west direction, parallel to the trend of nearby Marquette-Baraga dykes. **c, d, e)** Simplified cross-sections through the deposits showing the morphology of the Eagle and Eagle East intrusions and the distribution of mineralization. Locations of sections are shown on figure (b) (*after* Ding et al., 2010; Rose et al., 2018). **f, g)** Drill-core samples of typical Tamarack sulphide ore: (f) high-grade massive sulphides and (g) net-textured to semi-massive ore. In photograph (f) note the considerable pentlandite (brighter stringers) and chalcopyrite-cubanite (yellowish sulphides) content.

to the subhorizontal portion of the conduit, occurring close to the basal contact of the intrusion (Fig. 9e; Clow et al., 2017). The overlying funnel-shaped peridotite body contains negligible sulphide mineralization (Ding et al., 2010). The semi-massive to massive sulphide ores in both intrusions are characterized by elevated Ni/Cu ratios, relatively fractionated PGE patterns, and metal tenors comparable to those observed at Tamarack (Ding et al., 2012; Taranovic et al., 2016). Chalcopyrite-rich veins within the footwall show highly fractionated PGE patterns (Ding et al., 2012).

Within these conduit deposits, the addition of externally derived S is considered critical in producing the large sulphide accumulations characteristic of the Eagle deposits. Recent studies (e.g. Robertson et al., 2015) have shown that the addition of crustal S into these magmatic systems is controlled by the direct melting and assimilation of wall rock and xenoliths rather than through devolatilization reactions or dissolution of S in thermal aureoles. Thus, the Eagle and Eagle East ores are not considered to be contact-style deposits as external S is thought to have been derived distally from the present location of the ores. This notion is consistent with $\delta^{34}S$ and $\Delta^{33}S$ data of the sulphide ores, which indicate the addition of crustal-derived S, from both Paleoproterozoic and Archean sources distal to the deposits (Ding et al., 2012; Hink, 2016). The low $\delta^{34}S$ values ($\delta^{34}S$ 0–5 ‰) of the Eagle ores, which do not correspond to the high $\delta^{34}S$ values characteristic of the adjacent Michigamme Formation ($\delta^{34}S$ 4.6–29‰; Ding et al., 2012; Hink, 2016), could be attributed to selective assimilation of Michigamme Formation characterized by lower $\delta^{34}S$ values; isotopic exchange between the contaminated and pristine magma (Ripley and Li, 2003); or the extensive incorporation of Archean-derived S, as indicated by non-zero $\Delta^{33}S$ values (-0.86 to 0.86‰; Ding et al., 2012). Although isotopic data indicate <5% bulk contamination, possibly up to 20% locally, values are indicative of a contribution of S from country rocks of up to ~50% (Ding et al., 2012). Consequently, the sulphide liquid is viewed as being entrained and subsequently transported and deposited upwards through the magma conduit. Barnes et al. (2016) proposed, however, that the massive sulphide ores at Eagle accumulated as the result of the downward percolation of the sulphide liquid back into the former feeder dyke.

DISCUSSION

Onset of High-Volume Magmatism

As alluded to above, none of the new ages support an older and protracted onset of the main high-volume basaltic magmatism of the main MCR. All the ages of the Logan Sills (*sensu lato*) are compatible with a ca. 1106–1110 Ma onset, and the minor dispersion among the present ages (Table 2) may be in part analytical as uncertainties overlap. Only the reported date for olivine gabbro of the Kitto intrusion (*see* Fig. 1 for location), at 1117.5 ± 3.7 Ma (Heaman et al., 2007), remains as a suspected "outlier", and, hence, an important date we are still testing[4].

A sharp onset of the first high-volume basaltic magmatism sometime in the 1106 to 1110 Ma interval is also more in line with a similarly sharp onset of the main volcanic sequences at ca. 1107–1109 Ma[5], with the oldest recorded age being 1107.7 ± 1.9 Ma (Davis and Green, 1997) on a sample near the base of the volcanic sequence overlying the Puckwunge Sandstone along the Canada-USA border (Fig. 1), and a similar age of 1107.5 +4/-2 Ma for the base of the Osler Group (Davis and Sutcliffe, 1985).

This changed perspective on the older MCR units now draws renewed attention to the Echo Lake intrusion, a large layered gabbro complex with PGE mineralization buried below Jacobsville Sandstone on the southern flank of the MCR (Fig. 1). With a reported zircon age of 1110.8 ± 1.5 Ma on multiple near-concordant and concordant fractions (Cannon and Nicholson, 2001; S. Nicholson, pers. comm., 2018), this intrusion now stands as the oldest well dated intrusion in the MCR. As samples from this intrusion had robust zircons, new analysis of chemically abraded zircons may refine this age to better than 1 Myr precision.

Mineralized Mafic-Ultramafic Intrusion on the northern Flank of the Midcontinent Rift, Canada

On the northern flank of the MCR, north of Thunder Bay, there occur a number of localized mafic-ultramafic intrusions: the Thunder Bay North complex, including the chonolith-like Current Lake Intrusive Complex (with a narrow feeder and big bowl-shaped intrusion); the Sunday Lake intrusion; the Saturday Night intrusion; and the Thunder intrusion. All of these

[4] There are a few other older reported ages, either published or unpublished, but all are based on somewhat complicated and discordant baddeleyite data, such as the 1120 ± 4 Ma upper intercept age for a Baraga dyke near the Eagle deposit (Dunlop, 2013). Others are within error of a ca. 1109 Ma onset (e.g. Jackfish Island and other intrusions in Heaman et al., 2007).

[5] Note that in efforts to refine zircon ages on the volcanic sequences, using the latest innovations in high-precision U-Pb geochronology, there is a tendency towards reporting mean $^{206}Pb/^{238}U$ ages of multiple concordant zircon analyses, or concordia ages (e.g. Swanson-Hysell et al., 2019), which, in most cases, are just slightly younger than older $^{207}Pb/^{206}Pb$ ages on similar samples, thus shifting the age framework to slightly younger ages (by 1–2 Myr). This shift in absolute time is further magnified by using a modified U isotope ratio (Hiess et al., 2012).

intrude Archean basement of the Quetico Subprovince below the northern limb of the MCR, and all are variably mineralized. Some are being actively explored. They were discovered by probing distinct geophysical anomalies (reverse remanence magnetic anomalies), following the discovery in 2002 of high-grade Ni-Cu-PGE sulphide ore in another intrusion, the Eagle intrusion, on the south side of the MCR[6].

The larger bowl-shaped main parts of these various intrusive complexes typically show ultramafic cumulate rocks near the base, with or without basal sulphide mineralization, overlain by mafic cumulates that grade up into evolved monzogabbros underneath a chilled upper contact that shows extensive interaction with Archean roof rocks (e.g. Fig. 6b). The apparent negative magnetic anomalies associated with these intrusions, indicating a significant component of reverse paleomagnetic remanence, suggested that these intrusions were part of the early rift story. Few of them were dated, except for the Thunder intrusion (as part of a TGI-4 study; *see* Trevisan et al., 2015), which has a zircon age of 1108.0 ± 1.0 Ma. We therefore sampled the Current Lake intrusion of the Thunder Bay North Complex, the Sunday Lake intrusion, and the Saturday Night intrusion, two of which yielded good zircon and baddeleyite separates from evolved, coarsest grained samples of upper monzogabbros.

Baddeleyites (5 fractions) from the Sunday Lake intrusion yield a preliminary age of 1109.0 ± 1.3 Ma (weighted mean $^{207}Pb/^{206}Pb$ age); the Current Lake sample (from the Beaver Lake part of the intrusion), yields a 1106.6 ± 1.6 Ma age (upper intercept). It is too early to tell from these initial results (Table 2) whether the minor age dispersion is real or whether it reflects minor analytical differences (such as common Pb corrections on baddeleyites with lower radiogenic Pb content, or other complications). It is entirely possible that all these intrusions formed within a million years at ca. 1108 Ma. Given the shape of some of these intrusions, with tube-like conduits (i.e. “chonoliths”), it seems likely that they represent dynamic feeders to the major sill complexes on the northern flank of the MCR, and/or the lower parts of the basaltic volcanic sequences that may have extended well onto the northern flank of the MCR.

On the southern flank of the rift, the Eagle – Eagle East Complex and nearby intrusions also fall in this same older age group. We have newly dated one of these differentiated intrusions, the Bovine Igneous Complex), which yields a preliminary baddeleyite age of 1106.2 ± 1.3 Ma (Table 2). It seems likely that the linear array of intrusions, including Eagle and Bovine Igneous Complex, share a genetic relationship with major east-west-trending dykes of the Baraga-Marquette swarm, which still lack precise and concordant U-Pb ages in the published literature[7]. In detail, however, the Baraga-Marquette swarm shows at least two discrete trends (east-northeast, and east-southeast) and may represent more than one swarm and magmatic event.

Why the “Tadpole”-Shape? And Magma Flow/ Filling Direction?

A remarkable feature of the Current Lake and adjacent Steepledge Lake complexes is their composite shape with shallow dipping/plunging conduits in the north, widening into larger bowl-shaped intrusions to the southeast, over a distance of ~4 to 10 km. Even more remarkable is that the somewhat younger Tamarack Complex, hundreds of kilometres to the southwest in Minnesota, shows a similar morphology—a basic plan view that we refer to as a “tadpole”. Also, Sunday Lake shows this basic plan view, although less pronounced, with a conduit-like appendage on its northwest side (Fig. 7). In addition to sharing this basic “tadpole” shape, the intrusions show a similar orientation and asymmetry, with the larger bowl-shaped bodies offset to the southeast (i.e. the tadpoles seem to be swimming in the same direction!).

Part of the explanation could be gentle southeast-directed tilting (e.g. ~5º into the rift), which could expose a somewhat deeper feeder dyke progressively to the north. Almost certainly this is part of the explanation and naturally leads to the question of flow or filling direction. Currently there are no hard data on the flow direction in these complexes, but an overall magma flow from northern conduit-like feeders into larger bowl-shaped intrusions in the south is our preferred[8]. This suggests that the larger bowl-shaped intrusions are the down-stream part of the complex that slowly filled and expanded by roof uplift and stoping, while undergoing internal crystal settling (cumulates at the base) and differentiation.

If our interpretation of flow direction is correct, it would suggest that sulphide ores are most likely to have accumulated in two places: 1) where narrow conduit-like feeders widened and fed into larger bodies to the southeast, due to decreasing magma flow rates and rapidly reduced transport capacity; and 2) localized

[6] At Current Lake, part of the Thunder Bay North Complex, the discovery of mineralized boulders on the lakeshore also contributed to the discovery of the Current Lake mineralized intrusion (A. MacTavish, pers. comm., 2018).

[7] Dunlop (2013) presented an upper intercept age of 1120 ± 4 Ma based on three discordant baddeleyite fractions.

[8] At the Current Lake Intrusive Complex, Panoramic Resources has generally been entertaining an opposite flow direction, i.e. from the southeastern bowl-shaped intrusion into the northern conduit (A. MacTavish, pers. comm., 2018).

sulphide accumulations along the bottom of the main bowls, due to local gravity settling of sulphide droplets and pooling in local footwall depressions. Neither of these targets is easy to find, particularly at depth. These predictions can be compared with the drill-defined sections shown in Figures 6 to 9.

Younger Mineralized Intrusions: Tamarack, Duluth Complex, Crystal Lake

Tamarack

We sampled several phases of the large Tamarack Intrusive Complex in Minnesota, parts of which hosts high-grade massive to semi-massive and disseminated Ni-Cu-PGE sulphides. An earlier date from the northern dyke-like feeder of the complex was determined at 1105.6 ± 1.3 Ma, using sparse baddeleyite from a feldspathic peridotite (Goldner, 2011). This date is based on three clustered, slightly discordant (1.1–1.5%) fractions. Some of our samples are still in progress, but zircons from the differentiated upper part of the large "southern bowl" of the complex yielded excellent concordant and overlapping results (Fig. 5a), resulting in a concordia age of 1103.8 ± 0.9 Ma. This precise and concordant result indicates that the Tamarack Complex is clearly younger than the ca. 1106–1109 Ma group of intrusions north of Thunder Bay. It is possible that it represents a feeder to the nearby "Chengwatana volcanics" that fill the southern part of the MCR (Fig. 1), for which Wirth and Gehrels (1998) reported a U-Pb zircon age of 1102 ± 5 Ma. The multi-lobed morphology of the Tamarack Intrusive Complex, suggesting three different phases and a dynamic, perhaps longer lived intrusive history, is compatible with a dynamic feeder-type system (Goldner, 2011; Taranovic et al., 2015).

Duluth Complex

The next younger intrusive complex is that of the very large Duluth Complex (Miller et al., 2001, 2002) dated by multiple samples at 1098–1099 Ma (Paces and Miller, 1993; Hoaglund, 2010). It has been described by numerous authors and will not be dealt with here in any detail, except for a few brief comments:

1. As recently reviewed by Cawthorn and Miller (2018), early work on the Duluth Complex by Grout (1918), then referred to as the "Duluth gabbro", recognized it as "a large, lenticular, centrally sunken, generally concordant, intrusive mass, with its thickness approximately one-tenth to one-twentieth of its width or diameter". Grout (1918) introduced the term "lopolith" (from the Greek word "lopos" meaning shell or dish) and interpreted the Mellen Complex across the lake (Fig. 1), now known to be slightly older, as the southern limb of his "lopolith". As explained by Cawthorn and Miller (2018), the modern view of the Duluth Complex has evolved significantly and the term "lopolith" is no longer appropriate, not here and possibly not elsewhere either (e.g. Bushveld).
2. In the modern literature, the Duluth Complex is commonly referred to as a "large layered intrusion", the second largest in the world after the Bushveld Complex. Therefore, it is often thought of as a laterally extensive layered complex (like the Bushveld), but a more detailed look at the Duluth Complex (Miller et al., 2001, 2002) reveals that it is indeed a "complex" in the very sense of the word—i.e., made up of several, if not many, more localized magmatic chambers or sub-intrusions, each with a slightly different magmatic history. This makes lateral correlation and a full understanding of the Duluth Complex inherently more difficult, in addition to the extensive glacial cover, and locally steep topography and thick tree cover.
3. Although there were no historic mines, the complex has been explored for many decades following the discovery of Cu-sulphide mineralization by F.W. Childers in 1948. Since then, exploration has involved numerous drilling campaigns and sinking of exploration shafts (Miller et al., 2002; Miller, 2011). Some projects along the basal contact of the complex (*see* Fig. 1), involving some massive but mainly large-tonnage disseminated Cu-Ni-PGE sulphide ores, are now in a final exploration and permitting stage. They are likely to go into modern production in the near future, as large bulk mining operations, in part using the existing infrastructure of adjacent iron mines (PolyMet, 2019).
4. These deposits along the base of the complex are among the largest undeveloped Cu-Ni-PGE sulphide resources in the world (e.g. Miller, 2011; Miller and Nicholson, 2013).

Given its dynamic evolution of multiple sub-intrusions or magma chambers, it seems likely that the Duluth Complex acted as staging chambers and feeders to parts of the volcanic sequence of the North Shore Volcanic Group, before magma supply contracted into a narrower feeding zone along the lakeshore (*see* Fig. 1 and below).

Crystal Lake Intrusion

The Crystal Lake Intrusion is a y-shaped, multi-phase, gabbroic intrusion ~40 km southwest of Thunder Bay and has been the target of past and on-going exploration programs. A detailed overview of the intrusion is given in another contribution to this volume by Smith et al. (2020). The absolute and relative age of this intrusion has been under debate, since the area also hosts a number of other gabbroic or diabase intrusions (Geul, 1970, 1973), in particular: the Logan Sills; the north-

northwest-trending Cloud River dykes; a dense development of major north-northeast-trending, rift-parallel Pigeon River dykes; and the locally internally differentiated, ~100–200 m wide Mount Mollie dyke (e.g. Cundari, 2012). In the field, we have established the following sequence of events in this area:

1. *North-northwest-trending Cloud River dykes:* 30–100 m wide diabase dykes. Our preliminary results for these dykes, based on baddeleyite data, suggest an age of 1109.2 ± 2.9 Ma, in general agreement with, but more precise than, the earlier result reported by Hollings et al. (2010).
2. *Logan Sills:* an extensive diabase (with local granophyre) sill complex now dated at 1106.3 ± 2.0 Ma. Only north-northeast-trending Pigeon River dykes demonstrably cut the Logan sills[9].
3. *Northwest-trending Mt. Josephine dyke:* a very large dyke (~100 m wide) just across the Canada–USA border, trending at right angles to the ridges defined by the Pigeon River dykes. We determined a combined zircon and baddeleyite upper intercept age for this dyke of 1099.0 ± 1.2 Ma (Table 2), which suggests a connection to Duluth Complex magmatism.
4. *Densely developed north-northeast-trending Pigeon River dykes and sheets:* major diabase to gabbroic dykes (and some dipping sheets), locally with internal differentiation (Geul, 1970, 1973). In the field, we established that Pigeon River dykes cut and are chilled against Cloud River dykes and thus younger (Bleeker et al., 2019; Smith et al., 2019). Our current results for Pigeon River dykes cluster at 1096 Ma, which suggest a broad connection with the younger intrusions in the roof of the Duluth Complex, i.e. Beaver Bay Complex and Sonju Lake Intrusion (Fig. 1, Tables 1, 2); and, in particular, the "Beaver River Diabase" (Miller and Chandler, 1997; Doyle, 2016), for which Paces and Miller (1993) established a crystallization age of 1095.8 ± 1.2 Ma. Large Pigeon River dykes form major topographic ridges in the area around Crystal Lake and our observations suggest that these ridges do not transect the Crystal Lake Intrusive Complex. We have searched the area of the Crystal Lake Intrusion for younger crosscutting diabase dykes, a search that came up negative. Hence, given that the dense Pigeon River swarm comprises numerous large, subparallel dykes, representing multiple intrusive pulses, and taking current dating uncertainties into consideration, the overall life span of this swarm is likely 1097–1094 Ma.
5. *Mount Mollie dyke:* a large, somewhat curved, east- to east-northeast-trending, internally differentiated dyke, locally with a core of fine- to coarse-grained granophyre. It has often been interpreted as a feeder dyke to the Crystal Lake Intrusion. Instead, we presently consider this dyke to be a member of the Pigeon River swarm and note that some other wide Pigeon River dykes in the area also show minor internal differentiation, with local granophyre (Geul, 1970, 1973). Our preliminary data on samples from the Mount Mollie dyke indicate an age of 1096.3 ± 1.4 (Smith et al., 2020), which is indistinguishable from our present Pigeon River dating results (Table 2). We have no explanation for the much older date reported by Hollings et al. (2010). We have searched for crosscutting relationships but, to date, have not identified conclusive field relationships, except for thin north-northeast-trending dykelets (with chilled margins) intruding into the Mount Mollie dyke, in agreement with multiple magma pulses within the overall Pigeon River swarm.
6. *Crystal Lake Intrusion:* and finally, the multiple gabbroic phases of the Crystal Lake Intrusion, a major keel-shaped to dyke-like, composite, intrusive body of both homogeneous gabbro/troctolite and mineralized vari-textured gabbros (Smith et al., 2020), not crosscut at surface by any of the dykes described earlier (but *see* cross-sections in Smith et al., 2020). Our most conclusive U-Pb results, on mineralized vari-textured gabbro from the northern limb of the intrusion indicates a crystallization age of 1093.2 ± 1.2 Ma (Fig. 5b).

Our preliminary results and observations thus suggest that the dense Pigeon River swarm and younger Crystal Lake Intrusion correlate in a broad sense with the Beaver Bay and Sonju Lake complexes in the roof of the Duluth Complex, and that the Mount Mollie dyke is not the direct feeder to the Crystal Lake Intrusion, but rather slightly older and part of the overall Pigeon River event. Specifically, the Pigeon River swarm appears to be the northeastern continuation of the Beaver River Diabase. The Crystal Lake Intrusion, at ca. 1093 Ma, represents a final intrusive pulse of this overall 1097–1092 Ma magmatic phase, which is also well represented in the volcanic sequences of the MCR.

[9] Our preliminary age for the main (upper) Logan Sill at Mount MacKay is within error of other nearby results. One that is robust and precise is the zircon age for the "Swamper Lake monzogabbro" at 1107.0 ± 1.1 Ma (Davis and Green, 1997), just across the Canada–USA border. These same authors also recalculated the original "Logan Sill" age (obtained at Lake Nipigon) to 1108.2 ± 0.9 Ma and considered this the age of onset of voluminous mafic magmatism. All these key ages are within uncertainty.

A few other gabbroic intrusions with this relatively young age are the Blake Township gabbro (Heaman et al., 2007) and the gabbroic complexes intruding the Osler Group volcanic rocks, i.e. the Moss Lake Gabbro and St. Ignace Island Complex (Table 2, and references therein). The older Cloud River dykes, with their distinct north-northwest-trend, at high angles to the Pigeon River swarm, represent a different magmatic phase related to the onset of high-volume magmatism. These various ages and trends of associated dykes (i.e. principal stress directions) indicate a significant reorganization of the system occurred at ca. 1096 Ma.

Post-Duluth Complex Contraction of Magma Supply into the Central Rift

It is interesting to note that the rift-parallel Pigeon River dykes (1097–1094 Ma) and the various younger "post-Duluth Complex" gabbroic intrusions discussed above all occur closer to the northwestern shore of Lake Superior (Fig. 1), i.e. closer to the rift axis, than many of the older intrusions (e.g. Thunder Bay North Complex, Tamarack, etc.), suggesting that the focus of magmatism contracted into the central rift as the lithosphere thinned and rifted apart. The Pigeon River dyke swarm, and the Beaver River Diabase to the south (Miller and Chandler, 1997), likely are the surface expression of this more focussed, rift-parallel, trans-lithospheric feeder zone, which we here refer to as the "North Shore Magmatic Feeder Zone" (NSMFZ, identified in Figure 1 by the grey zones along the northern shore of Lake Superior)[10]. It seems likely that the major Pigeon River dykes and the NSMFZ may have fed thick lava flows as far away as the Keweenaw Peninsula. There, the thick Greenstone Flow (Portage Lake Group) has a U-Pb age of 1094.0 ± 1.5 Ma (Davis and Paces, 1990), an age that is, within uncertainty, coeval with the Pigeon River dykes and the more localized gabbroic intrusions that occur along its trend (e.g. Crystal Lake, Moss Lake). Doyle (2016) arrived at a similar conclusion but focussed on the Beaver River Diabase of the Beaver Bay Complex. Our conclusion would extend this feeder zone into a more extensive linear zone (NSMFZ). Doyle (2016) draws attention to the presence of very calcic plagioclase megacrysts in both the Beaver River Diabase, where they can be tied to large, lower crustal anorthosite xenoliths, and in the basalts of the Greenstone Flow. Large plagioclase megacrysts have also been noted in some Pigeon River dykes but require further study to determine their anorthite content and whether they are xenocrysts from a similar source.

Implications for Midcontinent Rift "Magmatic Stages"

Miller and Nicholson (2013) and other authors have divided the magmatic evolution of the MCR into various phases or stages. A full review of this important topic is beyond the scope of this report and should await the completion of all our dating results. Nevertheless, a few comments are in order. Their "Initiation Stage" (1115–1110 Ma) remains somewhat nebulous as some of the older ages have been revised, and others remain under discussion and to be tested. Beyond the problematic ca. 1110–1120 Ma baddeleyite ages, there are, however, various "precursor events", often alkaline, throughout the wider region (Fig. 1, Table 1), which need to be included in the overall consideration.

Also, as more precise ages emerge, some of their later stages, and particularly their age boundaries, will require some revision. The "Early Stage" of Miller and Nicholson (2013: 1110–1106 Ma) encompasses the onset of high-volume mafic magmatism, which is supported by our study, but the new Tamarack ages challenge the boundary of the following "Hiatus Stage (1106–1101 Ma). Perhaps more importantly, the new insights into the major Pigeon River swarm and younger gabbroic intrusions, and the reorganization into a linear magmatic feeder zone (NSMFZ), argue for a distinct 1097–1092 Ma stage, correlating with the eruption of the entire Portage Lake lava sequence. An unconformity may mark the beginning of this sequence (*see also* Swanson-Hysell, 2019).

Tholeiitic Versus Alkaline Intrusion and Mantle Sources

With more complete and accurate age control, and the spatial distribution of intrusions, as shown in Figure 1, an interesting aspect of the overall MCR evolution is the predominance of alkaline intrusions in the eastern part of the rift. The well dated Coldwell Complex (Heaman and Machado, 1992; G. Dunning and D. Good, pers. comm., 2017), and also the reasonably well dated Nemegosenda alkaline complex farther east (Heaman et al., 2007), overlap in age with the 1106–1110 Ma onset of high-volume basaltic magmatism but are compositionally distinct from the mafic-ultramafic intrusions in the western MCR. Many of the low-volume, alkaline precursor events (e.g. Great Abitibi swarm, and various lamprophyric to kimberlitic intrusions) are also concentrated in the eastern part (Fig. 1). This spatial dichotomy may speak to the nature of the underlying mantle lithosphere as well as issues discussed below.

[10] The presence of this zone is probably also the reason why the northwest shore of Lake Superior is overall more linear as compared to, for instance, the southern shore of Lake Superior.

Mantle Plume Centre and Potential Plume Track?

With the overall diversity of intrusions, and the various dyke swarms of different trends but in many cases still with poorly defined ages, we caution against drawing any simple radiating patterns that might indicate a hypothetical centre of mantle plume impact. The Great Abitibi dyke swarm (1141 Ma: Krogh et al, 1987) has featured prominently in such conjecture (Ernst and Buchan, 1997) but is much older than many dyke swarms proximal to the MCR, such as the rift-parallel Pigeon River swarm (1096 Ma: this study), and pre-dates high-volume mafic magmatism by >30 Myr. Also, the evidence for lateral emplacement of the main Great Abitibi dyke, from a magmatic source south of the MCR (Ernst, 1990), should be treated as speculative at this stage. The Kipling dyke, which perhaps may define a fanning pattern and plays an important role in this debate, has no U-Pb age. Furthermore, in this general area east and northeast of the MCR, both ca. 2110 Ma Marathon dykes and ca. 2170 Ma Biscotasing dykes have similar northeast-trends and complicate the tracing of MCR-related dykes, and associated paleopoles are not fully distinct (e.g. Great Abitibi poles and Biscotasing poles overlap). Clearly, more complete and precise ages, as well as compositional data, on many of the dyke swarms of the MCR are needed to better infer overall emplacement patterns and define the entire tectonomagmatic system and its evolution.

To determine a possible centre of plume impact, and a potential plume track, it is also important to zoom out to the full scale of the North American continent (and beyond, Rodinia) and to consider all the mafic magmatism on a >1000 km scale that could be related (Table 1). To highlight the potential scale of MCR-related magmatism, some of the key pulses of magmatic activity, at ca. 1160 Ma and 1108 Ma, are echoed as far away as northern Saskatchewan in the form of diabase intrusions in the Athabasca sandstone basin (French et al., 2002; Bleeker and Chamberlain, 2015). Are these separate events or are they distant manifestations of the same overall tectonomagmatic system? Similarly, the southwestern arm of the MCR, extending far into the mid-continent, may be connected with the essentially contemporaneous southwest USA diabase province (Hammond, 1990; Bright et al., 2014). It is interesting to note that this latter magmatic province may extend to somewhat younger ages than the MCR (e.g. Heaman and Grotzinger, 1992), perhaps providing a hint of a plume track. Any such speculation would also need to be reconciled against the paleomagnetic data and apparent polar wander path derived from the MCR (Swanson-Hysell et al., 2019). Finally, in this overall context, it is worth drawing attention to the study of Edwards and Blackburn (2018), who recorded a distinct 1.1 Ga heating pulse at the base of the lithosphere (from xenoliths in the Victor kimberlite) far to the northeast of Lake Superior (~600 km) in the James Bay Lowlands.

CONCLUSIONS

Our ongoing research has added critical details, field observations, and U-Pb data to the magmatic evolution of the MCR, with new high-precision U-Pb ages for ~10 of the mineralized intrusions and associated feeder dyke swarms, while a number of samples is still in progress. Our results favour a relatively sharp onset of high-volume basaltic magmatism at ca. 1106–1110 Ma in the main part of the rift, with coeval more alkaline magmatism in the eastern MCR. Only the older date on the Kitto intrusion (ca. 1117 Ma: Heaman et al., 2007) in the Lake Nipigon area remains as an older age “outlier”, one that we are still testing.

The mineralized Sunday Lake Intrusion, north of Thunder Bay, dated at 1109.0 ± 1.3 Ma, is one of the oldest differentiated intrusions on the northern flank of the MCR. On the southern flank, the large Echo Lake layered intrusion has the oldest robust zircon age of 1110.8 ± 1.5 Ma (Cannon and Nicholson, 2001), and for this reason alone should be a target for age refinement using modern chemical abrasion-isotope dilution-thermal ionization mass spectrometry (CA-ID-TIMS) methods, especially as it is known to contain relatively good zircons.

Mineralized intrusions of the MCR do not all fall in this early age group, but show a temporal distribution that correlates with all the main volcanic phases of the rift. Through time, they can be grouped as follows:

1. Early MCR intrusions, ca. 1110–1106 Ma: Sunday Lake, Thunder, Thunder Bay North (Current Lake), and many of the intrusion on the southern flank, such as Eagle, Bovine Igneous Complex, and Echo Lake; also the large Coldwell Complex.
2. The Tamarack Intrusive Complex at ca. 1105–1103 Ma.
3. The Mellen Complex at ca. 1102 Ma[11].
4. The main part of the Duluth Complex at 1099 Ma.
5. Younger intrusions along the northwestern shore of Lake Superior at ca. 1097–1094 Ma: Beaver Bay and Sonju Lake intrusions and the main Pigeon River dykes, including Mount Mollie at 1096 Ma.
6. Crystal Lake Intrusion at ca. 1094–1092 Ma.

[11] This large complex on the southern flank of the MCR has not been a focus of our study, but clearly could benefit from age refinement. Could it be coeval with the Duluth Complex, as Grout (1918) initially inferred, both emplaced near the base of the overlying volcanic sequences?

All of the mineralized intrusions that so far have received detailed studies appear more complex than single-phase intrusions and all are part of dynamic feeder systems that likely fed coeval parts of the volcanic stratigraphy of the rift. Hence, there is scope for detailed geochemical and isotopic studies (e.g. *see* Doyle, 2016) to reveal some of these connections in more detail and to better understand the overall dynamics.

As the age database improves, it is clear that the focus of magmatic activity, including emplacement of mineralized intrusions, contracted into the developing rift after the emplacement of the Duluth Complex. The major rift-parallel ca. 1096 Ma Pigeon River swarm, in particular, marks this contraction into a major feeder zone along the northwest shore of Lake Superior (our NSMFZ), perhaps stretching from the Duluth Complex in the southwest all the way to St. Ignace Island in the northeast. The southwest-trending Carlton dykes (Fig. 1) may extend this zone farther to the southwest. This zone and its major dykes likely were the major fissure system that fed the entire 1097–1092 Ma Portage Lake lava pile, including the thick Greenstone Flow. Following multiple pulses of dyke emplacement into the NSMFZ, this feeder zone was then intruded by several more localized gabbroic complexes, such as Crystal Lake.

Finally, at the higher precision that is likely to advance understanding of rift processes (~1 Myr or better), a number of challenging geochronology-related problems remain, first among which are the remaining discordance in some of the data (Fig. 4) and the sometimes minor offset of slightly discordant baddeleyite data to marginally older $^{207}Pb/^{206}Pb$ ages as compared to zircon data (Fig. 10). This offset was first noted decades ago in Nipigon sills (Davis and Sutcliffe, 1985); it also revealed itself in the data for the Thunder intrusion (Trevisan et al., 2015), and it is also present in some of our data. We are still working on this problem, but it is one reason to keep searching for well behaved zircons that respond well to chemical abrasion. Another approach would be to identify samples with relatively robust baddeleyite populations that could withstand air abrasion. This could test whether this issue with baddeleyite is related to the surface of the crystals or to other factors.

In comparison, a minor problem is the tendency in modern high-precision U-Pb dating to concentrate on potentially more precise $^{206}Pb/^{238}U$ data from multiple overlapping concordant zircon analyses (e.g. Swanson-Hysell et al., 2019), which typically are slightly younger than $^{207}Pb/^{206}Pb$ upper intercept ages on similar samples, creating an offset among data sets. Similarly, switching to a more refined U isotopic ratio amplifies this offset (Hiess et al., 2012). This may be useful in terms of the best possible absolute age control on key units of the MCR, but it complicates correlation between data sets and published ages at a ~1–2 Myr time scale for an area such as the MCR.

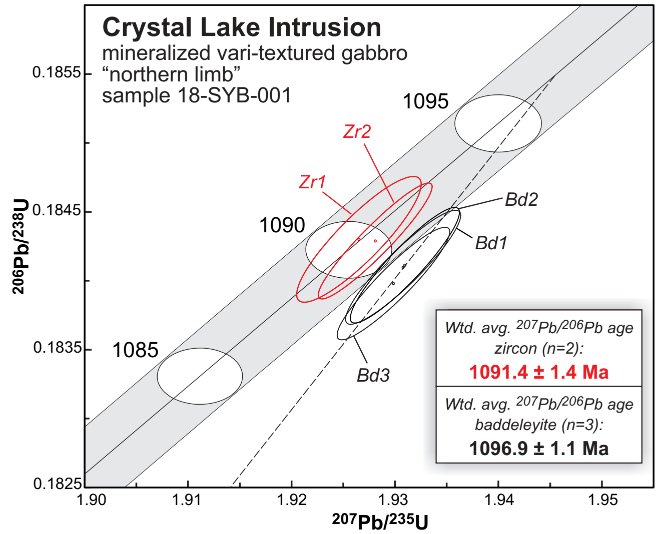

Figure 10. Standard U-Pb concordia diagram showing an example of the relative offset of baddeleyite data (n = 3, black ellipses) with respect to zircon (n = 2, red ellipses). The apparent offset to the right results in older $^{207}Pb/^{206}Pb$ ages for the baddeleyite, well beyond the uncertainties of the individual analyses. Several factors could contribute to this offset, some of which are presently not fully understood in each case study. It remains as a significant hindrance to obtaining accurate and highly precise ages on zircon-poor rock units (e.g. many diabase dykes). The example shown is from the unmineralized troctolite of the northern limb of the Crystal Lake Intrusion, but this issue is known to occur in many Midcontinent Rift data sets, including high-resolution data on zircon and baddeleyite standards from the Duluth Complex (K. Chamberlain, pers. comm., 2019). All data-point error ellipses are 2σ.

ACKNOWLEDGMENTS

This report is a contribution to NRCan's Targeted Geoscience Initiative Program (TGI). Support for this study was provided through the Orthomagmatic Ni-Cu-PGE-Cr Ore Systems Project's 'Activity NC-1.3: Controls on the localization and timing of mineralized intrusions in intra-continental rift systems, with a specific focus on the ca. 1.1 Ga Mid-continent Rift system'. The authors thank our partners at Rio Tinto (Dean Rossell, Brian Goldner, Justin Laberge), North American Palladium (Steve Flank, Dave Peck), Transition Metals (Grant Mourre, Scott McLean), Panoramic (Al McTavish), and Stillwater Canada (Dave Good, John McBride) for their help, access to drill core, and constructive discussions. Terry Boerboom from the Minnesota Geological Survey is thanked for his detailed knowledge of and input on Minnesota geology, in the field and otherwise, and Jim Miller for various discussions on MCR geology.

Colleagues from the USGS (Klaus Schultz, Suzanne Nicholson) provided key information on units in Michigan and Wisconsin, and shared the unpublished data on the Echo Lake intrusion. Reviews by Terry Boerboom and Tony LeCheminant improved the manuscript. Valérie Bécu assisted with the technical editing and Elizabeth Ambrose took care of final editing and correction of minor imperfections. Both are thanked for their skillful assistance. Last but not least, members of the TGI-5 team are thanked for taking care of a thousand little tasks from general project management to outreach and consultations, without which none of this research could have proceeded. Thank you all.

REFERENCES

Alibert, C. and Albarede, F., 1988. Relationships between mineralogical, chemical and isotopic properties of some North American kimberlites; Journal of Geophysical Research, v. 93, p. 7643–7671.

Allen, D.J., Hinze, W.J., Dickas, A.B., and Mudrey, M.G., Jr., 1997. Integrated geophysical modeling of the North American Midcontinent Rift System: New interpretations for western Lake Superior, northwestern Wisconsin, and eastern Minnesota; *in* Middle Proterozoic to Cambrian Rifting, Central North America, (ed.) R.J. Ojakangas, A.B. Dickas, and J.C. Green; Geological Society of America, Special Paper 312, p. 47–72.

Ames, D.E., Kjarsgaard, I.M., McDonald, A.M., and Good, D.J., 2017. Insights into the extreme PGE enrichment of the W Horizon, Marathon Cu-Pd deposit, Coldwell Alkaline Complex, Canada: Platinum-group mineralogy, compositions and genetic implications; Ore Geology Reviews, v. 90, p. 723–747.

Barnes, S.J., Cruden, A.R., Arndt, N., and Saumur, B.M., 2016. The mineral system approach applied to magmatic Ni–Cu–PGE sulphide deposits; Ore geology reviews, v. 76, p. 296–316.

Bell, K. and Blenkinsop, J., 1980. Ages and initial 87Sr/86Sr ratios from alkali complexes of Ontario; *in* Geoscience Research Grant Program, Summary of Research 1979–1980, (ed.) E.G. Pye; Ontario Geological Survey, Miscellaneous Paper 93, p. 16–23.

Bleeker, W. and Chamberlain, K., 2015. Robust U-Pb age for the Douglas River dyke, Athabasca Basin – Further indications of a significant magmatic event in western Laurentia at 1165 Ma; *in* Reconstruction of supercontinents back to 2.7 Ga using the Large Igneous Province (LIP) Record: With implications for mineral deposit targeting, hydrocarbon exploration, and Earth system evolution – Year 5 Confidential Summary for Project Sponsors, (ed.) R.E. Ernst and W. Bleeker; Report A203, 9 p.

Bleeker, W., Liikane, D.A., Smith, J., Hamilton, M., Kamo, S.L., Cundari, R., Easton, M., and Hollings, P., 2018. Activity NC-1.3: Controls on the localisation and timing of mineralized intrusions in intra-continental rift systems, with a specific focus on the ca. 1.1 Ga Mid-continent Rift (MCR) system; *in* Targeted Geoscience Initiative: 2017 Report of Activities, Volume 2, (ed.) N. Rogers; Geological Survey of Canada, Open File 8373, p. 15–27.

Bleeker, W., Hamilton, M., Kamo, S., Liikane, D., Smith, J., Hollings, P., Cundari, R., Easton, M., and Davis, D., 2019. High-resolution dating of the magmatic plumbing system of the Midcontinent Rift System—Insights into rift evolution and mineralization processes; Institute on Lake Superior Geology Proceedings, 51st Annual Meeting, Abstracts and Proceedings, v. 65, p. 10–11.

Boerboom, T.J., Wirth, K.R., and Evers, J.F., 2014. Five newly acquired high-precision U-Pb age dates in Minnesota, and their geologic implications; *in* Institute on Lake Superior Geology Proceedings, 60th Annual Meeting, Abstracts and Proceedings, v. 60, pt. 1, p. 13–14.

Bornhorst, T.J. and Barron, R.J., 2011. Copper deposits of the western Upper Peninsula of Michigan; *in* Archean to Anthropocene: Field Guides to the Geology of the Mid-Continent of North America, (ed.) J.D. Miller, G.J. Hudak, C. Wittkop, and P.I. McLaughlin; Geological Society of America, Field Guide 24, p. 83–99. https://doi.org/10.1130/2011.0024(05)

Bright, R.M., Amato, J.M., Denyszyn, S.W., and Ernst, R.E., 2014. U-Pb geochronology of 1.1 Ga diabase in the southwestern United States: Testing models for the origin of a post-Grenville large igneous province; Lithosphere, v. 6, p. 135–156.

Cannon, W.F., 1992. The Midcontinent rift in the Lake Superior region with emphasis on its geodynamic evolution; Tectonophysics, v. 213, p. 41–48.

Cannon, W.F. and Nicholson, S.W., 2001. Geology map of the Keweenaw Peninsula and adjacent area; U.S. Geological Survey, Geological Investigations Series, Map I-2696, scale 1:100 000.

Chaffee, M.R., 2015. Petrographic and geochemical study of the hybrid rock unit associated with the Current Lake Intrusive Complex; M.Sc. thesis, University of Minnesota, Minneapolis, Minnesota, 139 p.

Clow, G.G., Normand L.L., Rennie, D.W., and Scholey, B.J.Y., 2017. Technical Report on the Eagle Mine, Michigan, U.S.A, NI 43-101 Report; Roscoe Postle Associates Inc. for Lundin Mining Corporation. <www.lundinmining.com/site/assets/files/2640/2017-04-26-eagle-ni-43-101.pdf[accessed December 1, 2019]

Cogulu, E.H., 1993a. Factors controlling postcumulus compositional changes of chrome-spinels in the Crystal Lake Intrusion, Thunder Bay, Ontario; Geological Survey of Canada, Open File 2748, 77 p.

Cogulu, E.H., 1993b. Mineralogy and chemical variations of sulphides from the Crystal Lake Intrusion, Thunder Bay; Ontario. Geological Survey of Canada, Open File 2749, 52 p.

Cawthorn, R.G. and Miller, J., 2018. Lopolith–A 100 year-old term. Is it still definitive?; South African Journal of Geology, v. 121, p. 253–260.

Cundari, R., 2012. Geology and geochemistry of Midcontinent Rift-related igneous rocks; M.Sc. thesis, Lakehead University, Thunder Bay, Ontario, 142 p.

Currie, K.L., 1976. The alkaline rocks of Canada; Geological Survey of Canada, Bulletin 239, 228 p., incl. Map 1369A, scale 1:5 000 000.

D'Angelo, M., 2013. Mineralogy, petrology and geochemistry of the Steepledge Intrusion; B.Sc. thesis, Lakehead University, Thunder Bay, Ontario, 83 p.

Davis, D.W. and Green, J.C., 1997. Geochronology of the North American Midcontinent rift in western Lake Superior and implications for its geodynamic evolution; Canadian Journal of Earth Sciences, v. 34, p. 476–488.

Davis, D.W. and Paces, J.B., 1990. Time resolution of geologic events on the Keweenaw Peninsula and implications for development of the Midcontinent Rift system; Earth and Planetary Science Letters, v. 97, p. 54–64.

Davis, D.W. and Sutcliffe, R.H., 1985. U-Pb ages from the Nipigon plate and northern Lake Superior; Geological Society of America Bulletin, v. 96, p. 1572–1579.

Ding, X., Li, C., Ripley, E.M., Rossell, D., and Kamo, S., 2010. The Eagle and East Eagle sulfide ore-bearing mafic-ultramafic intrusions in the Midcontinent Rift System, Upper Michigan: Geochronology and petrologic evolution; Geochemistry, Geophysics, Geosystems, v. 11, 22 p.

Ding, X., Ripley, E.M., and Li, C., 2012. PGE geochemistry of the Eagle Ni–Cu–(PGE) deposit, Upper Michigan: Constraints on ore genesis in a dynamic magma conduit; Mineralium Deposita, v. 47, p. 89–104.

Donoghue, K.A., Ripley, E.M., and Li, C., 2014. Sulfur isotope and mineralogical studies of Ni-Cu sulfide mineralization in the Bovine Igneous Complex intrusion, Baraga Basin, Northern Michigan; Economic Geology, v. 109, p. 325–341.

Doyle, M.S., 2016. Geologic and geochemical attributes of the Beaver River Diabase and Greenstone Flow: Testing a possible intrusive-volcanic correlation in the 1.1 Ga Midcontinent Rift; M.Sc. thesis, University of Minnesota, Duluth, Minnesota, 176 p.

Drenth, B.J., Anderson, R.R., Schulz, K.J., Feinberg, J.M., Chandler, V.W., and Cannon, W.F., 2015. What lies beneath: geophysical mapping of a concealed Precambrian intrusive complex along the Iowa–Minnesota border; Canadian Journal of Earth Sciences, v. 52, p. 279–293.

Dunlop, M., 2013. The Eagle Ni-Cu-PGE magmatic sulfide deposit and surrounding mafic dikes and intrusions in the Baraga Basin, Upper Michigan: Relationships, petrogenesis and implications for magmatic sulfide exploration; M.Sc. thesis, Indiana University, Bloomington, Indiana, 93 p.

Edwards, G.H. and Blackburn, T., 2018. Detecting the extent of ca. 1.1 Ga Midcontinent Rift plume heating using U-Pb thermochronology of the lower crust; Geology, v. 46, p. 911–914.

Emst, R.E., 1990. Magma flow directions in two mafic Proterozoic dyke swarms of the Canadian Shield: As estimated using anisotropy of magnetic susceptibility data; *in* Mafic dykes and Emplacement Mechanisms, (ed.) A.J. Parker, P.C. Rickwood, and D.H. Tucker; Balkema, Rotterdam, p. 231–235.

Ernst, R.E. and Buchan, K.L., 1997. Giant radiating dyke swarms: their use in identifying pre-Mesozoic large igneous provinces and mantle plumes; American Geophysical Union, Geophysical Monograph 100, p. 297–334.

Fairchild, L.M., Swanson-Hysell, N.L., Ramezani, J., Sprain, C.J., and Bowring, S.A., 2017. The end of Midcontinent Rift magmatism and the paleogeography of Laurentia; Lithosphere, v. 9, p. 117–133.

Flank, S., 2017. The petrography, geochemistry and stratigraphy of the Sunday Lake Intrusion, Jacques Township, Ontario; M.Sc. thesis, Laurentian University, Sudbury, Ontario, 71 p.

Fletcher, T., Peters, O., and Thomas B., 2018. Second Independent Technical Report on the Tamarack North Project – Tamarack, Minnesota, NI 43-101 Technical Report; DRA Americas Inc. for Talon Metals Corp., 213 p. <https://talonmetals.com/wp-content/uploads/2018/10/20180326_Talon_Tamarack_NI_43-101.pdf> [accessed December 1, 2019]

Foley, D.J., 2011. Petrology and Cu-Ni-PGE mineralization of the Bovine Igneous Complex, Baraga County, Northern Michigan; M.Sc. thesis, University of Minnesota, Minneapolis, Minnesota, 109 p.

French, J.E., Heaman, L.M., and Chacko, T., 2002. Feasibility of chemical U–Th–total Pb baddeleyite dating by electron microprobe; Chemical Geology, v. 188, p. 85–104.

Geul, J.J.C., 1970. Geology of Devon and Pardee Townships and the Stuart Location, District of Thunder Bay; Ontario Department of Mines, Geological Report 87, 58 p.

Geul, J.J.C., 1973. Geology of Crooks Township, Jarvis and Prince Locations, and Offshore Islands, District of Thunder Bay; Ontario Department of Mines, Geological Report 102, 46 p.

Giguerre, J.F., 1975 Geology of St. Ignace Island and Adjacent Islands, District of Thunder Bay; Ontario Division of Mines, Geological Report 118, 35 p. Accompanied by Map 2285, scale 1:63 360 or l inch to l mile.

Gittins, J., Macintyre, R.M., and York, D., 1967. The ages of carbonatite complexes in eastern Canada; Canadian Journal of Earth Sciences, v. 4, p. 651–655.

Goldner, B.D., 2011. Igneous petrology of the Ni-Cu-PGE mineralized Tamarack intrusion, Aitkin and Carlton Counties, Minnesota; M.Sc. thesis, University of Minnesota, Minneapolis, Minnesota, 156 p.

Good, D.J. and Crocket, J.H., 1994. Genesis of the Marathon Cu-platinum-group element deposit, Port Coldwell alkalic complex, Ontario; a Midcontinent rift-related magmatic sulfide deposit; Economic Geology, v. 89, p. 131–149.

Good, D.J., Epstein, R., McLean, K., Linnen, R.L., and Samson, I.M., 2015. Evolution of the Main Zone at the Marathon Cu-PGE sulfide deposit, Midcontinent Rift, Canada: Spatial relationships in a magma conduit setting; Economic Geology, v. 110, p. 983–1008.

Good, D.J., Cabri, L.J., and Ames, D.E., 2017. PGM facies variations for Cu-PGE deposits in the Coldwell Alkaline Complex, Ontario, Canada; Ore Geology Reviews, v. 90, p. 748–771.

Goodgame, V.R., Johnson, J.R., MacTavish, A.D., Stone, W.E., Watkins, K.P., and Wilson, G.C., 2010. The Thunder Bay North Deposit: Chonolith-hosted Pt-Pd-Cu-Ni mineralization related to the Midcontinent Rift; *in* Abstracts; 11th International Platinum Symposium, Extended Abstracts, p. 21–24.

Green, J.C., 1983. Geologic and geochemical evidence for the nature and development of the Middle Proterozoic (Keweenawan) Midcontinent Rift of North America; Tectonophysics, v. 94, p. 413–437.

Green, J.C., Bornhorst, T.J., Chandler, V.W., Mudrey, M.G., Jr., Myers, P.R., Pesonen, L.V., and Wilband, J.T., 1987. Keweenawan dykes of the Lake Superior region: Evidence for the evolution of the Middle Proterozoic Midcontinent Rift of North America; *in* Mafic Dyke Swarms, (ed.) H.C. Hall and W.F. Fahrig; Geological Association of Canada, Special Paper 34, p. 289–302.

Grout, F.F., 1918. The lopolith; an igneous form exemplified by the Duluth gabbro; American Journal of Science, v. 46, p. 516–22.

Hammond, J.G., 1990. Middle Proterozoic diabase intrusions in the southwestern U.S.A. as indicators of limited extensional tectonism; *in* Mid-Proterozoic Laurentia-Baltica, (ed.) C.F. Gower, T. Rivers, and B. Ryan; Geological Association of Canada, Special Paper 38, p. 517–531.

Hanson, R.E., Crowley, J.L., Bowring, S.A., Ramezani, J., Gose, W.A., Dalziel, I.W., Pancake, J.A., Seidel, E.K., Blenkinsop, T.G., and Mukwakwami, J., 2004. Coeval large-scale magmatism in the Kalahari and Laurentian cratons during Rodinia assembly; Science, v. 304, p. 1126–1129.

Hart, T.R. and MacDonald, C.A., 2007. Geology and structure of the western margin of the Nipigon Embayment; Canadian Journal of Earth Sciences, v. 44, p. 1021–1040.

Hart, T.R. and Magyarosi, Z., 2004. Precambrian geology of the northern Black Sturgeon River and Disraeli Lake area, Nipigon Embayment, northwestern Ontario; Ontario Geological Survey, Open File 6138, 56 p.

Hart, T.R., terMeer, M., and Jolette, C., 2002. Precambrian geology of Kitto, Eva, Summers, Dorothea and Sandra townships, northwestern Ontario–Phoenix Bedrock Mapping Project; Ontario Geological Survey, Open File 6095, 206 p.

Hauck, S.A., Severson, M.J., Zanko, L., Barnes, S.J., Morton, P., Alminas, H., Foord, E.E., and Dahlberg, E.H., 1997. An overview of the geology and oxide, sulfide, and platinum-group element mineralization along the western and northern contacts of the Duluth Complex; *in* Middle Proterozoic to Cambrian Rifting, Central North America, (ed.) R.W. Ojakangas, A.B. Dickas, and J.C. Green; Geological Society of America, Special Paper 312, p. 137–185.

Heaman, L.M. and Grotzinger, J.P., 1992. 1.08 Ga diabase sills in the Pahrump Group, California: Implications for development of the Cordilleran miogeocline; Geology, v. 20, p. 637–640.

Heaman, L.M. and Machado, N., 1992. Timing and origin of mid-continent rift alkaline magmatism, North America: evidence from the Coldwell Complex; Contributions to Mineralogy and Petrology, v. 110, p. 289–303.

Heaman, L.M., Kjarsgaard, B.A., and Creaser, R.A., 2004. The temporal evolution of North American kimberlites; Lithos, v. 76, p. 377–397.

Heaman, L.M., Easton, R.M., Hart, T.R., Hollings, P., MacDonald, C.A., and Smyk, M., 2007. Further refinement to the timing of Mesoproterozoic magmatism, Lake Nipigon region, Ontario; Canadian Journal of Earth Sciences, v. 44, p. 1055–1086.

Heggie, G.J., 2005. Whole rock geochemistry, mineral chemistry, petrology and Pt, Pd mineralization of the Seagull intrusion, Northwestern Ontario; M.Sc. thesis, Lakehead University, Thunder Bay, Ontario, 156 p.

Hiess, J., Condon, D.J., McLean, N., and Noble, S.R., 2012. $^{238}U/^{235}U$ systematics in terrestrial uranium-bearing minerals; Science, v. 335, p. 1610–1614.

Hink, B.D., 2016. Geochemical and Petrological Studies on the Origin of Nickel-Copper Sulphide Mineralization at the Eagle Intrusion in the Marquette County, Michigan; M.Sc. thesis, Western Michigan University, Kalamazoo, Michigan, 129 p.

Hoaglund, S., Miller, J.D., Crowley, J.L., and Schmitz, M.D., 2010. U-Pb zircon geochronology of the Duluth Complex and related hypabyssal intrusions: Investigating the emplacement history of a large multiphase intrusive complex related to the 1.1 Ga Midcontinent Rift; Institute on Lake Superior Geology Proceedings, 56th Annual Meeting, Abstracts and Proceedings, v. 56, pt. 1, p. 25–26.

Hollings, P., Hart, T., Richardson, A., and MacDonald, C.A., 2007. Geochemistry of the Mesoproterozoic intrusive rocks of the Nipigon Embayment, northwestern Ontario: evaluating the earliest phases of rift development; Canadian Journal of Earth Sciences, v. 44, p. 1087–1110.

Hollings, P., Smyk, M., Heaman, L.M., and Halls, H., 2010. The geochemistry, geochronology, and paleomagnetism of dikes and sills associated with the Mesoproterozoic Midcontinent Rift near Thunder Bay, Ontario, Canada; Precambrian Research, v. 183, p. 553–571.

Hutchinson, D., White, R., Cannon, W., and Schulz, K., 1990. Keweenaw hot spot: Geophysical evidence for a 1.1 Ga mantle plume beneath the Midcontinent Rift system; Journal of Geophysical Research, v. 95, p. 10 869–10 884.

Jirsa, M.A., Boerboom, T.J., Chandler, V.W., Mossler, J.H., Runkel, A.C., and Setterholm, D.R., 2011. S-21 Geologic map of Minnesota – bedrock geology; Minnesota Geological Survey, University of Minnesota Digital Conservancy <https://conservancy.umn.edu/handle/11299/101466> [accessed December 1, 2019].

Kaminsky, F.V., Sablukov, S.M., Sablukova, L.I., and Shchukin, V.S., 2000. Petrology of kimberlites from the newly discovered Whitefish Lakefield in Ontario; GeoCanada 2000: the Millennium Geoscience Summit Conference CD, Abstract no. 1203.

Kent, R.W., Storey, M., and Saunders, A.D., 1992. Large igneous provinces: Sites of plume impact or plume incubation?; Geology, v. 20, p. 891–894.

Koerber, A. and Thakurta, J., 2017. Geochemical and petrological investigation of the prospective Ni-Cu-PGE mineralization at the Echo Lake intrusion in the upper peninsula of Michigan, USA; Geological Society of America Annual Meeting, Abstracts with Programs, v. 49. https://doi.org/10.1130/abs/2017AM-304314

Krogh, T.E., Corfu, F., Davis, D.W., Dunning, G.R., Heaman, L.M., Kamo, S.L., Machado, N., Greenough, J.D., and Nakamura, E., 1987. Precise U-Pb isotopic ages of diabase dykes and mafic to ultramafic rocks using trace amounts of baddeleyite and zircon; *in* Mafic Dyke Swarms, (ed.) H.C. Halls and W.F. Fahrig; Geological Association of Canada, Special Paper 34, p. 147–152.

Laarman, J.E., 2007. Geochemistry and PGE mineralization of the Kitto intrusion: A product of Mesoproterozoic plume magmatism through fault bounded Archean crust, east Nipigon Embayment, northern Ontario; M.Sc. thesis, Lakehead University, Thunder Bay, Ontario, 276 p.

Lauerma, R., 1995. Kursun ja Sallan kartta-alueiden kallioperä. Summary: Pre-Quaternary rocks of the Kursu and Salla map-sheet areas; Geological map of Finland, scale 1:100 000, Explanation to the map of Pre-Quaternary Rocks, Sheets 3643, 4621, 4623.

Lawson, A.C., 1893. The laccolith sill of the north-west coast of Lake Superior; Geological and Natural History Survey of Minnesota, Bulletin No. 8, Section II, p. 24–48.

Ludwig, K.R., 1998. On the treatment of concordant uranium-lead ages; Geochimica et Cosmochimica Acta, v. 62, p. 665–676.

Ludwig, K.R., 2003. User's manual for Isoplot 3.00: A geochronological toolkit for Microsoft Excel; Berkeley Geochronology Center, Special Publication No. 4, 71 p.

Mattinson, J.M., 2005. Zircon U/Pb chemical abrasion (CA-TIMS) method: Combined annealing and multi-step partial dissolution analysis for improved precision and accuracy of zircon ages; Chemical Geology, v. 220, p. 47–66.

McCormick, K.A., Chamberlain, K.R., and Paterson, C.J., 2017. U-Pb baddeleyite crystallization age for a Corson diabase intrusion: possible Midcontinent Rift magmatism in eastern South Dakota; Canadian Journal of Earth Sciences, v. 55, p. 111–117.

Miller, J.D., 1998. Potential for reef-type PGE mineralization in the Duluth Complex: Evidence from the Layered Series at Duluth; The Minnesota Prospector, Special Issue, p. 8–12.

Miller, J.D., 2011. Geology and mineral deposits of the Duluth Complex, Minnesota; United States Geological Survey. <https://mn.water.usgs.gov/projects/tesnar/2011/Presentations/Miller DC%20Min_USGS%20workshop.pdf> [accessed December 1, 2019]

Miller, J.D., 2016. Geology of the Endion Sill, Duluth; Institute on Lake Superior Geology, Proceedings - Field Trips, v. 62, pt. 2, p. 80–101.

Miller, J.D. and Chandler, V.W., 1997. Geology, petrology, and tectonic significance of the Beaver Bay Complex, northeastern Minnesota; *in* Middle Proterozoic to Cambrian Rifting, Central North America, (ed.) R.W. Ojakangas, A.B. Dickas, and J.C. Green; Geological Society of America, Special Paper 312, p. 73–96.

Miller, J.D. and Nicholson, S.W., 2013. Geology and mineral deposits of the 1.1 Ga Midcontinent Rift in the Lake Superior region – An overview; *in* Field Guide to the Cu-Ni-PGE Deposits of the Lake Superior Region, (ed.) J.D. Miller; Precambrian Research Center Guidebook 13-1, p. 1–50.

Miller, J.D., Jr., Green, J.C., Severson, M.J., Chandler, V.W., and Peterson, D.M., 2001. Geologic map of the Duluth Complex and related rocks, northeastern Minnesota; Minnesota Geological Survey, Miscellaneous Map M-119, scale 1:200 000.

Miller, J.D., Jr., Green, J.C., Severson, M.J., Chandler, V.W., Hauck, S.A., Peterson, D.M., and Wahl, T.E., 2002. Geology and mineral potential of the Duluth Complex and related rocks of northeastern Minnesota; Minnesota Geological Survey, Report of Investigations 58, 207 p.

Mitchell, R.H., Platt, R.G., and Cheadle, S.P., 1983. A gravity study of the Coldwell Complex, northwestern Ontario and its petrological significance; Canadian Journal of Earth Sciences, v. 20, p. 1631–1638.

Mitchell, R.H., Platt, R.G., Lukosius-Sanders, J., Artist-Downey, M., and Moogk-Pickard, S., 1993. Petrology of syenites from center III of the Coldwell alkaline complex, northwestern Ontario, Canada; Canadian Journal of Earth Sciences, v. 30, p. 145–158.

Morris, W.J., 1977. Geochemistry and origin of the Yellow Dog Plains peridotite, Marquette Country, Northern Michigan; M.S. thesis. Michigan State University, East Lansing, Michigan.

Mungall, J.E., Kamo, S.L. and McQuade, S., 2016. U-Pb geochronology documents out-of-sequence emplacement of ultramafic layers in the Bushveld Igneous Complex of South Africa; Nature Communications, v. 7, 13 p. https://doi.org/10.1038/ncomms13385

Nicholson, S.W., Cannon, W.F., and Schulz, K.J., 1992. Metallogeny of the Midcontinent rift system of North America; Precambrian Research, v. 58, p. 355–386.

Ojakangas, R.W. and Morey, G.B., 1982. 7A: Keweenawan prevolcanic quartz sandstones and related rocks of the Lake Superior region; *in* Geology and Tectonics of the Lake Superior Basin, (ed.) R.J. Wold and W.J. Hinze; Geological Society of America, Boulder, Colorado, Memoir 156, p. 85–96.

Ontario Geological Survey, 1991a. Bedrock map of Ontario, east-central sheet; Ontario Geological Survey, Map 2543, scale 1: 1 000 000.

Ontario Geological Survey, 1991b. Bedrock map of Ontario, west-central sheet; Ontario Geological Survey, Map 2542, scale 1: 1 000 000.

Osamani, L.A., 1991. Proterozoic mafic dike swarms in the Superior Province; *in* Geology of Ontario, (ed.) P.C. Thurston, H.R. Williams, R.H. Sutcliffe, and G.M. Stott; Ontario Geological Survey, Special Volume 4, Part 1, p. 661–681.

Paces, J.B. and Miller, J.D., 1993. Precise U-Pb ages of Duluth complex and related mafic intrusions, northeastern Minnesota: Geochronological insights to physical, petrogenetic, paleomagnetic, and tectonomagmatic processes associated with the 1.1 Ga midcontinent rift system; Journal of Geophysical Research: Solid Earth, v. 98, p. 13 997–14 013.

Platt, R.G. and Mitchell, R.H., 1979. The Marathon Dikes. I: Zirconium-rich titanian garnets and manganoan magnesian ulvoespinel-magnetite spinels; American Mineralogist, v. 64, p. 546–550.

Platt, R.G. and Mitchell, R.H., 1982. The Marathon Dikes: ultrabasic lamprophyres from the vicinity of McKellar Harbour, NW Ontario; American Mineralogist, v. 67, p. 907–916.

Platt, R.G., Mitchell, R.H., and Holm, P.M., 1983. Marathon dikes: Rb–Sr and K–Ar geochronology of ultrabasic lamprophyres from the vicinity of McKellar Harbour, northwestern Ontario, Canada; Canadian Journal of Earth Sciences, v. 20, p. 961–967.

PolyMet, 2019. The NorthMet Project Overview. <https://polymet-mining.com/operations/northmet-snapshot/> [accessed December 1, 2019]

Queen, M., Hanes, J.A., Archibald, D.A., Farrar, E., and Heaman, L.M., 1996. 40Ar/39Ar phlogopite and U–Pb perovskite dating of lamprophyre dykes from the eastern Lake Superior region: evidence for a 1.14 Ga magmatic precursor to Midcontinent Rift volcanism; Canadian Journal of Earth Sciences, v. 33, p. 958–965.

Queffurus, M. and Barnes, S.J., 2014. Selenium and sulfur concentrations in country rocks from the Duluth Complex, Minnesota, USA: Implications for formation of the Cu-Ni-PGE sulphides; Economic Geology, v. 109, p. 785–794.

Ripley, E.M., 2014. Ni-Cu-PGE mineralization in the Partridge River, South Kawishiwi, and Eagle intrusions: A review of contrasting styles of sulfide-rich occurrences in the Midcontinent rift system; Economic Geology, v. 109, p. 309–324.

Ripley, E.M. and Li, C., 2003. Sulfur isotope exchange and metal enrichment in the formation of magmatic Cu-Ni-(PGE) deposits; Economic Geology, v.98, p. 635–641.

Ripley, E.M., Taib, N.I., Li, C., and Moore, C.H., 2007. Chemical and mineralogical heterogeneity in the basal zone of the Partridge River Intrusion: implications for the origin of Cu–Ni sulphide mineralization in the Duluth Complex, midcontinent rift system; Contributions to Mineralogy and Petrology, v. 154, p. 35–54.

Robertson, J., Ripley, E.M., Barnes, S.J., and Li, C., 2015. Sulfur liberation from country rocks and incorporation in mafic magmas; Economic Geology, v. 110 p. 1111–1123.

Rose, K., Essig, W., and Thakurta, J., 2018. Variation trends in sulphide isotope ratios at the Eagle and East Eagle intrusions and the surrounding country and basement rocks of the Baraga Basin, Upper Peninsula, Michigan; Institute of Lake Superior Geology, 64th Annual Meeting, Abstracts, p. 87.

Rukhlov, A.S. and Bell, K., 2010. Geochronology of carbonatites from the Canadian and Baltic Shields, and the Canadian Cordillera: Clues to mantle evolution; Mineralogy and Petrology, v. 98, p. 11–54.

Sage, R.P., 1985. Geology of carbonatite-alkalic rock complexes of Ontario: Chipman Lake Area. Districts of Thunder Bay and Cochrane; Ontario Ministry of Northern Affairs and Mines, Ontario Geological Survey, Study 44, 44 p.

Sage, R.P., 1987a. Geology of carbonatite-alkalic rock complexes in Ontario: Nemegosenda Lake Alkalic Rock Complex. District of Sudbury; Ontario Ministry of Northern Development and Mines, Ontario Geological Survey, Study 34, 132 p.

Sage, R.P., 1987b. Geology of carbonatite-alkalic rock complexes in Ontario: Shenango Township Alkalic Rock Complex. District of Sudbury and Algoma; Ontario, Ministry of Northern Development and Mines, Ontario Geological Survey, Study 35, 119 p.

Sage, R.P., 1987c. Geology of carbonatite-alkalic rock complexes in Ontario: Big Beaver House Carbonatite Complex. District of Kenora; Ontario Ministry of Northern Development and Mines, Ontario Geological Survey, Study 51, 71 p.

Sage, R.P., 1988a. Geology of carbonatite-alkalic rock complexes in Ontario: Seabrook Lake Carbonatite Complex. District of Algoma; Ontario Ministry of Northern Development and Mines, Ontario Geological Survey, Study 31, 45 p.

Sage, R.P., 1988b. Geology of carbonatite-alkalic rock complexes in Ontario: Clay-Howells Alkalic Rock Complex. District of Sudbury and Algoma; Ontario Ministry of Northern Development and Mines, Ontario Geological Survey, Study 37, 104 p.

Sage, R.P., 1988c. Geology of carbonatite-alkalic rock complexes in Ontario: Valentine Township Carbonatite Complex. District of Cochrane; Ontario Ministry of Northern Development and Mines, Ontario Geological Survey, Study 39, 37 p.

Sage, R.P., 1988d. Geology of carbonatite-alkalic rock complexes of Ontario: Killala Lake Alkalic Rock Complex. District of Thunder Bay; Ministry of Northern Development and Mines, Ontario Geological Survey, Study 45, 120 p.

Sage, R.P., 1988e. Geology of carbonatite-alkalic rock complexes in Ontario: Firesand River Carbonatite Complex. District of Algoma; Ontario Ministry of Northern Development and Mines, Ontario Geological Survey, Study 47, 82 p.

Sage, R.P., 1988f. Geology of carbonatite-alkalic rock complexes in Ontario: Schryburt Lake Carbonatite Complex. District of Kenora; Ontario Ministry of Northern Development and Mines, Ontario Geological Survey, Study 50, 43 p.

Sage, R.P., 1991. Alkaline rocks, carbonatite and kimberlite complexes of Ontario, Superior Province; *in* Geology of Ontario, Ontario Geological Survey, Special Volume 4, p. 683–709.

Salminen, J., Pesonen, L.J., Mertanen, S., Vuollo, J., and Airo, M.L., 2009. Palaeomagnetism of the Salla diabase dyke, northeastern Finland, and its implication for the Baltica-Laurentia entity during the Mesoproterozoic; Geological Society, London, Special Publications, v. 323, p. 199–217.

Schoene, B., Crowley, J.L., Condon, D.J., Schmitz, M.D., and Bowring, S.A., 2006. Reassessing the uranium decay constants for geochronology using ID-TIMS U-Pb data; Geochimica et Cosmochimica Acta, v. 70, p. 426–445.

Severson, M.J., Miller, J.D., Peterson, D.M., Green, J.C., Hauck, S.A., Chandler, V.W., and Wahl, T.E., 2002. Mineral potential of the Duluth Complex and related intrusions. Geology and Mineral Potential of the Duluth Complex and Related Rocks of Northeastern Minnesota; Minnesota Geological Survey, Report of Investigations 58, p. 164–200.

Shirey, S.B., 1997. Re-Os isotopic compositions of Midcontinent rift system picrites: implications for plume–lithosphere interaction and enriched mantle sources; Canadian Journal of Earth Sciences, v. 34, p. 489–503.

Smith, J., Bleeker, W., Liikane, D.A., Hamilton, M., Cundari, R., and Hollings, P., 2019. Characteristics of Ni-Cu-PGE sulphide mineralization within the 1.1 Ga Midcontinent Rift; *in* Targeted Geoscience Initiative: 2018 report of activities, (ed.) N. Rogers; Geological Survey of Canada, Open File 8549, p. 421–432.

Smith, J.W., Bleeker, W., Hamilton, M., Petts, D., Kamo, S.L., and Rossell, D., 2020. Timing and controls on Ni-Cu-PGE mineralization within the Crystal Lake Intrusion, 1.1 Ga Midcontinent Rift; *in* Targeted Geoscience Initiative 5: Advances in the understanding of Canadian Ni-Cu-PGE and Cr ore systems – Examples from the Midcontinent Rift, the Circum-Superior Belt, the Archean Superior Province, and Cordilleran Alaskan-type intrusions, (ed.) W. Bleeker and M.G. Houlé; Geological Survey of Canada, Open File 8722, p. 37–63.

Smyk, M.C. and Franklin, J.M., 2007. A synopsis of mineral deposits in the Archean and Proterozoic rocks of the Lake Nipigon Region, Thunder Bay District, Ontario; Canadian Journal of Earth Sciences, v. 44, p. 1041–1053.

Smyk, M.C., Hollings, P., and Heaman, L.M., 2006. Preliminary investigations of the petrology, geochemistry and geochronology of the St. Ignace Island Complex, Midcontinent Rift, northern Lake Superior, Ontario; Institute of Lake Superior Geology, 52nd Annual Meeting, Proceedings and Abstracts, v. 52, p. 61–62.

Smyk, M.C. and Hollings, P., 2009. Mesoproterozoic Midcontinent Rift-related mafic intrusions near Thunder Bay: Update; *in* Summary of Field Work and Other Activities 2009, Ontario Geological Survey, Open File Report 6240, p. 11–15.

Stein, C.A., Stein, S., Elling, R., Keller, G.R., and Kley, J., 2018a. Is the “Grenville Front” in the central United States really the Midcontinent Rift?; GSA Today, v. 28, p. 4–10.

Stein, S., Stein, C.A., Elling, R., Kley, J., Keller, G.R., Wysession, M., Rooney, T., Frederiksen, A., and Moucha, R., 2018b. Insights from North America's failed Midcontinent Rift into the evolution of continental rifts and passive continental margins; Tectonophysics, v. 74, p. 403–421.

Stone, D., Kamineni, D.C., and Jackson, M.C., 1992. Precambrian geology of the Atikokan area, northwestern Ontario; Geological Survey of Canada, Bulletin 405, 115 p., 1 sheet. https://doi.org/10.4095/134053 (this publication contains Stone, D, and Kamineni, D.C., 1989. Geology, Atikokan area, Ontario; Geological Survey of Canada, Map 1666A, scale 1:50 000).

Sutcliffe, R.H., 1986. The petrology, mineral chemistry and tectonics of Proterozoic rift-related igneous rocks at Lake Nipigon, Ontario; Ph.D. thesis, University of Western Ontario, London, Ontario, 326 p.

Swanson-Hysell, N.L., Burgess, S.D., Maloof, A.C., and Bowring, S.A., 2014. Magmatic activity and plate motion during the latent stage of Midcontinent Rift development; Geology, v. 42, p. 475–478.

Swanson-Hysell, N.L., Ramezani, J., Fairchild, L.M., and Rose, I.R., 2019. Failed rifting and fast drifting: Midcontinent Rift development, Laurentia’s rapid motion and the driver of Grenvillian orogenesis; Geological Society of America Bulletin, v. 131, p. 913–940. https://doi.org/10.1130/B31944.1

Taranovic, V., Ripley, E.M., Li, C., and Rossell, D., 2015. Petrogenesis of the Ni–Cu–PGE sulfide-bearing Tamarack Intrusive Complex, Midcontinent Rift System, Minnesota; Lithos, v. 212, p. 16–31.

Taranovic, V., Ripley, E.M., Li, C., and Rossell, D., 2016. Chalcophile element (Ni, Cu, PGE, and Au) variations in the Tamarack magmatic sulfide deposit in the Midcontinent Rift System: implications for dynamic ore-forming processes; Mineralium Deposita, v. 51, p. 937–951.

Taranovic, V., Ripley, E.M., Li, C., and Shirey, S.B., 2018. S, O, and Re-Os isotope studies of the Tamarack Igneous Complex: melt-rock interaction during the early stage of Midcontinent Rift development; Economic Geology, v. 113, p. 1161–1179.

Thomas, D.G., Melnyk, J., Gormely, L., Searston, S., and Kulla, G., 2011. Magma Metals Limited, Thunder Bay North polymetallic project, Ontario, Canada, NI 43-101 Technical Report on Preliminary Assessment; AMEC Americas Ltd for Magma Metals Ltd, p. 10-14 – 10-18. <https://www.miningdataonline.com/reports/Thunder_Bay_North_2011_PEA.pdf> [accessed December 1, 2019]

Trevisan, B.E., 2014. The petrology, mineralization and regional context of the Thunder mafic to ultramafic intrusion, Midcontinent Rift, Thunder Bay, Ontario; M.Sc. thesis, Lakehead University, Thunder Bay, Ontario, 285 p.

Trevisan, B.E., Hollings, P., Ames, D.E., and Rayner, N.M., 2015. The petrology, mineralization, and regional context of the Thunder mafic to ultramafic intrusion, Midcontinent Rift, Thunder Bay, Ontario; *in* Targeted Geoscience Initiative 4: Canadian nickel-copper-platinum group elements-chromium ore systems – fertility, pathfinders, new and revised models, (ed.) D.E. Ames and M.G. Houlé: Geological Survey of Canada, Open File 7856, p. 139–149.

Van Schmus, W.R., 1992. Tectonic setting of the Midcontinent Rift System; Tectonophysics, v. 213, p. 1-15.

Van Schmus, W.R. and Hinze, W.J., 1985. The midcontinent rift system; Annual Review of Earth and Planetary Sciences, v. 13, p. 345–383.

Vervoort, J.D. and Wirth, K.R., 2004. Origin of the rhyolites and granophyres of the Midcontinent Rift, northeast Minnesota. Institute on Lake Superior Geology Proceedings, 50th Annual Meeting, 52nd Annual Meeting, Proceedings and Abstracts, v. 52, p. 160–161.

Vervoort, J., Wirth, K., Kennedy, B., Sandland, T., and Harpp, K., 2007. The magmatic evolution of the Midcontinent Rift: New geochronologic and geochemical evidence from felsic magmatism; Precambrian Research, v. 157, p. 235–268.

Weiblen, P.W., 1982. 6: Keweenawan intrusive igneous rocks; *in* Geology and Tectonics of the Lake Superior Basin, (ed.) R.J. Wold and W.J. Hinze; Geological Society of America, Boulder, Colorado, Memoir 156, p. 57–82.

Weiblen, P.W., Mathez, E.A., and Morey, G.B., 1972. Logan intrusions; *in* Geology of Minnesota: A Centennial Volume, (ed.) P.K. Sims and G.B. Morey; Minnesota Geological Survey, St. Paul, Minnesota, p. 394–410.

Wirth, K.R. and Gehrels, G.E., 1998. Precise U–Pb zircon ages of Midcontinent rift rhyolite (Chengwatana Volcanics), Clam Falls, WI; Institute on Lake Superior Geology, Proceedings, v. 44, pt. 1, p. 124-125.

Wold, R.J. and Hinze, W.J., 1982. Geology and Tectonics of the Lake Superior Basin; Geological Society of America, Boulder, Colorado, Memoir 156, 280 p.

Wu, F.Y., Mitchell, R.H., Li, Q.L., Zhang, C., and Yang, Y.H., 2017. Emplacement age and isotopic composition of the Prairie Lake carbonatite complex, Northwestern Ontario, Canada; Geological Magazine, v. 154, p. 217–236.

Zartman, R.E., Nicholson, S.W., Cannon, W.F., and Morey, G., 1997. U-Th-Pb zircon ages of some Keweenawan Supergroup rocks from the south shore of Lake Superior; Canadian Journal of Earth Science, v. 34, p. 549–561.